Distribution Agreement

Signature:

______________________________ _______________

Futu Chen Date

Analyzing Uncertainties in Estimating $PM_{2.5}$- and O_3-Related Human Health Outcomes in the Mainland China Due to Emission Scenarios, Concentration Response Functions, and Other Assumptions

By

Futu Chen
Master of Public Health

Environmental Health

Eri Saikawa, PhD
Committee Chair

Paige Tolbert, PhD
Committee Member

Analyzing Uncertainties in Estimating $PM_{2.5}$- and O_3-Related Human Health Outcomes in the Mainland China Due to Emission Scenarios, Concentration Response Functions, and Other Assumptions

By

Futu Chen

B.E.
Shanghai University
2014

Thesis Committee Chair: Eri Saikawa, PhD

An abstract of
A thesis submitted to the Faculty of the
Rollins School of Public Health of Emory University
in partial fulfillment of the requirements for the degree of
Master of Public Health
in Environmental Health
2016

Abstract

Analyzing Uncertainties in Estimating $PM_{2.5}$- and O_3-Related Human Health Outcomes in the Mainland China Due to Emission Scenarios, Concentration Response Functions, and Other Assumptions
By Futu Chen

Background: Exposures to fine particulate matter (particulate matter with an aerodynamic diameter of less than or equal to 2.5 μm; $PM_{2.5}$) as well as ground-level ozone (O_3) are associated with a variety of adverse health effects. Ambient air pollutants are also anticipated to continuously affect large populations in China in the future. However, although several assumptions affect the estimation of potential future health outcomes, only a few studies have discussed the associated uncertainties.

Objectives: Our goal is to assess the sensitivity of $PM_{2.5}$- and O_3-related human health outcomes to emission scenarios and to concentration-response (C-R) functions, as well as population projections, when estimating health outcomes.

Methods: We used the Weather Research and Forecasting model coupled with Chemistry (WRF-Chem) to simulate $PM_{2.5}$ and O_3 concentrations and conducted base year simulations for the year 2008 and future simulations for 2050. We used three different emission inventories for the base year and four scenarios for 2050. We applied population-weighted concentrations to quantify the change in exposure at the individual level between the base year and the future and applied the C-R function to project the pollutant-related mortality and morbidity. An analysis of variance was used to quantify uncertainty and to apportion the uncertainty to different inputs.

Results: Our research results show a decrease in mortality and morbidity in 2050 due to an up to 80% decrease in population-weighted $PM_{2.5}$ concentration in the cold season and an up to 20% decrease in population-weighted O_3 concentration in the summer in 2050, compared to the base year. 5-37% increase in O_3 in January in 2050 led to excess mortality and morbidity. We found that the major source of uncertainty (74%) came from present emissions when projecting $PM_{2.5}$-related health outcomes in January. Future emission scenarios contributed up to 79% uncertainty in O_3-related health outcome estimations in July.

Conclusion: Our results illustrate that the source and the magnitude of emissions have a great impact on premature mortality and morbidity calculations. Our results also highlight the importance of using an ensemble approach to assess future air pollution-related health outcomes.

Analyzing Uncertainties in Estimating $PM_{2.5}$- and O_3-Related Human Health Outcomes in the Mainland China Due to Emission Scenarios, Concentration Response Functions, and Other Assumptions

By

Futu Chen

B.E.
Shanghai University
2014

Thesis Committee Chair: Eri Saikawa, PhD

A thesis submitted to the Faculty of the
Rollins School of Public Health of Emory University
in partial fulfillment of the requirements for the degree of
Master of Public Health
in Environmental Health
2016

Acknowledgements

I would first like to extend my thanks to my amazing and excellent thesis advisor, Dr. Eri Saikawa, for all of her help and guidance. I am deeply grateful to Dr.

Min Zhong for her very valuable inputs. Thanks to Dr. Stefanie Ebelt Sarnat, for her advice on my proposal. I would like to acknowledge Dr. Yang Liu, Jessica Belle, Qingyang Xiao for their valuable inputs, Jacqueline Jaryi Yap for her review on my poster. I am also thankful to Dr. Saikawa's air quality group, for all their supports.

Finally, I am grateful to my family, for their love and continuous support.

This research used population data from LandScan 2008™. This product was made utilizing the LandScan 2008™ High Resolution global Population Data Set copyrighted by UT-Battelle, LLC, operator of Oak Ridge National Laboratory under Contract No. DE-AC05-00OR22725 with the United States Department of Energy. The United States Government has certain rights in this Data Set. Neither UT-BATTELLE, LLC NOR THE UNITED STATES DEPARTMENT OF ENERGY, NOR ANY OF THEIR EMPLOYEES, MAKES ANY WARRANTY, EXPRESS OR IMPLIED, OR ASSUMES ANY LEGAL LIABILITY OR RESPONSIBILITY FOR THE ACCURACY, COMPLETENESS, OR USEFULNESS OF THE DATA SET.

Table of Contents

Section 1: Background ... **1**

1.1 $PM_{2.5}$ and O_3 Exposure ... 1

1.2 Air Quality in China ... 2

1.3 Concentration-response (C-R) Function ... 4

1.4 Air Quality Modeling and Uncertainty ... 5

Section 2:Methods ... **8**

2.1 $PM_{2.5}$ and O_3 Concentration Estimation ... 8

2.2 Study Population ... 10

2.3 $PM_{2.5}$ and O_3 Population-Weighted Concentration Estimation ... 11

2.4 C-R Function and Health Impact Estimation ... 12

2.5 Sensitivity Analysis ... 14

Section 3: Results ... **15**

3.1 National Air quality Characteristics ... 15

3.2 Population-weighted concentrations ... 18

3.3 Health estimates ... 22

3.4 Uncertainty and sensitivity analysis ... 24

Section 4: Discussions ... **28**

Section 5: Conclusions and Recommendations ... **31**

References ... **32**

Tables and Figures ... **40**

Appendices ... **57**

Section 1: Background

1.1 $PM_{2.5}$ and O_3 exposure

Short-term and long-term exposures to fine particulate matter (particulate matter with an aerodynamic diameter less than or equal to 2.5 µm; $PM_{2.5}$) as well as ground-level ozone (O_3) are associated with a variety of adverse health effects (WHO 2014; Kappos et al. 2004). Many of the epidemiological studies in the United States have discussed this association (eg. Levy et al. 2005; Correia et al. 2013; Hajat et al. 2015; Hoek et al. 2013). The Six Cities Study (Dockery et. al, 1993) demonstrated that the long-term $PM_{2.5}$ exposure is tightly associated with mortality with a 26% excess risk in all-cause mortality when comparing the most polluted city (Steubenville, Ohio) to the least polluted one (Portage, Wisconsin). Franklin et al. (2007) did a cohort study at a community level and documented a 1.21% excessed risk of all-cause mortality from a 10 $\mu g/m^3$ increase in ambient $PM_{2.5}$ exposure. There is sufficient evidence linking $PM_{2.5}$ exposure and cardiovascular and respiratory diseases at an individual level with the affected population ranging from children to the elderly (Kampa and Elias, 2008). Weichenthal et al. (2013) reviewed studies on $PM_{2.5}$ and related cardiovascular and respiratory health effects and found both epidemiological and biological connections between them. Air pollutants, such as PM, will stimulate the body to produce reactive oxygen species (ROS) as its biological response, and this PM-oxidative burden can be one of the mediators of cardiovascular disease (Strak et al. 2012; Tonne et al. 2012). In addition, studies also found gene-environmental interactions between ambient $PM_{2.5}$ and high-frequency heart rate variability (HRV). Most of the studies concluded a negative effect between high ambient $PM_{2.5}$ exposure and low HRV (Weichenthal et al. 2013).

The epidemiological evidence for O_3 exposure is also linked to adverse health effects. The National Mortality and Morbidity Air Pollution Study (NMMAPS, 2000) found the positive association between O_3 and daily mortality when the O_3 levels were highest. In terms of morbidity, Halonen et al. (2009) published a 12.6% increase in asthma-chronic obstructive pulmonary disease (COPD) hospital admissions for children, and a 6.4% increase for elderly compared with the previous day O_3 level and adjusting for $PM_{2.5}$.

1.2 Air quality in China

China has long been criticized for its air pollution. According to the Word Bank's statistics, China's population was the highest in the world (1,364,270,000) in 2014, followed by India (1,295,292,000) and the United States (318,857,000). There is a large population exposed to high levels of PM as well as O_3 in the ambient air that does not meet either the Chinese ambient air quality standard (GB 3095-1996) or the World Health Organization Air Quality Guidelines (Table 1) (Ministry of Environmental Protection of People's Republic of China, 1996; WHO 2005; Zhang et al., 2010). In a recent report by GreenPeace, the annual mean $PM_{2.5}$ concentrations in total 366 cities in China were 50.2 $\mu g/m^3$ in 2015 with the highest annual mean of 80.7 $\mu g/m^3$ in Henan, and lowest annual mean of 10.6 $\mu g/m^3$ in Tibet (GreenPeace, 2016). *China Daily* also reported 9.6% higher $PM_{2.5}$ concentrations in 2015 in the North China compared to the previous winter when people used more heating (China Daily, 2016). This article also pointed out that 8-hour daily average O_3 concentrations in 2015 was 3.4% and 7.9% higher compared to the years 2013 and 2014, respectively (China Daily, 2016).

Because of an increasing awareness of air pollution by the public since the 2008 Olympic Games and the 2010 World Expo, a new draft of criteria pollutant standards came out in

2012 and took effect in January, 2016. This new draft added annual and 24-hour mean $PM_{2.5}$ concentrations in the NAAQS (GB 3095-2012) (Table 1). The new standard also required all the counties in the nation to report their daily air quality. To test this policy, several key regions, including Beijing-Tianjin-Hebei, the Yangtze River Delta, the Pearl River Delta, and provincial capitals were required to publicize air quality data since 2012. Based on the data published on the Chinese Environmental Protection Bureau website, it is clear that most of the big cities will fail to meet the new $PM_{2.5}$ standard (MEP, 2016). Chan and Yao (2008) analyzed air pollution in multiple urban cities in China and they concluded that PM pollution was severe, as well as secondary pollution (such as O_3). Cao et al. (2011) conducted the first epidemiological cohort study focusing on air pollution and mortality in China at the national level. They studied total suspended particles (TSP), sulfur dioxide (SO_2) and nitrogen oxides (NO_x), and found a 0.9% increase for all-cause mortality with 10 $\mu g/m^3$ increase in TSP, a 1.8% increase for mortality with 10 $\mu g/m^3$ increase in SO_2, and a 1.5% growth with 10 $\mu g/m^3$ increase in NO_x.

Anthropogenic emissions are the major source of ambient air pollution in China (Chan and Yao, 2008). The key source of energy in China is coal and the burning of coal, along with industrial production, is the primary PM emissions source. Huang et al. (2014) assessed the sources of various air pollutant emissions in China and suggested that in addition to the control on primary particulate emissions, the reduction of secondary aerosol precursor emissions is necessary. Zhang et al. (2011) found that the source of air pollution in Beijing has gradually transformed from coal burning to motor vehicle emissions. Vehicle exhausts in the future will also speed photochemical reaction, which will result in higher O_3 formation.

1.3 Concentration-response (C-R) function

Concentration-response (C-R) function is a dose-response relationship that measures how changes in the dose of exposure is associated with the alterations in health endpoints (EPA, 2015). Over the last decades, researchers have developed several C-R functions to describe air pollution and its impact on population health (Sujaritpong et al., 2014; Pope et al., 2015). Most of the research proved that the shape of the curve is not linear, but closer to log linear because of the risk associated with cigarette smoking (Daniels et al. 2000; Pope et al. 2009). Pope et al. (2015) explored the application of C-R function and suggested the usage of C-R function on projecting the health impacts of air pollution. While most of the studies were conducted in the US, the generalizability of these C-R functions remains in question. This is especially the case for China. Although there is one published study analyzing the national scale long-term chronic exposure to ambient air pollution in China, the author did not include $PM_{2.5}$ and O_3 in their analyses due to the lack of exposure data (Cao, 2011). Previously-published papers discussed the pollution-related health problems using the pollution data from unofficial monitoring sites (You, 2014). Most of the air pollution epidemiological studies in China discussed TSP and O_3, in individual cities (Chang et al. 2003; Kan et al. 2007; T.W. Wong et al. 2002; T.W. Wong et al. 2008). The lack of available data and studies made the construction of C-R function for China a difficult task.

In the Harvard China Project, Lei (2013) established C-R functions of $PM_{2.5}$ and O_3 pollution on both chronic and acute health outcomes for China for the first time, based on the epidemiological studies in multiple Chinese cities, as well as in the U.S. In addition, they discussed the difference in $PM_{2.5}$ concentrations between the U.S. and China, and adjusted the Risk Ratio (RR) from these studies. We used their C-R function for health outcomes estimation at the national and the regional level in China in this study.

1.4 Air quality modeling and uncertainty

To estimate health outcomes, we explored the potential impacts of emissions on the formation of $PM_{2.5}$ and O_3 concentrations. We used the Weather Research and Forecasting model with Chemistry (WRF-Chem) to simulate air quality. Chemical reactions in the atmosphere and meteorology both affect the formation of air pollutants. As suggested by Seaman (2000), we used a model that couples meteorology and chemistry.

However, model simulation is not a cure-all solution. The model prediction results are influenced by both emission scenarios and meteorological factors (Akimoto, 2003). Emission inventory inputs for generating current and future air quality have been discerned as the most pressing factor for describing future air quality issues (Lin et al., 2005). Emissions in Asia are especially not well understood. Studies have been done to compare emission inventories for Asia and found large discrepancies (Saikawa et al. 2014). For the Regional Emission Inventory in Asia version 2 (REAS) and the Emissions Database for Global Atmospheric Research version 4.2 (EDGAR), Zhong et al. (2015) found a 40-70% difference between REAS and EDGAR when predicting surface PM_{10} concentrations, and a 16–20 % difference when estimating O_3 mixing ratios.

Although previous studies have compared uncertainties among emission inventories, relatively fewer investigations have been done to understand how these uncertainties will affect the health outcomes (Morita et al. 2014; Lelieveld et al. 2015; Knowlton et al. 2004; Post et al. 2012; Kim et al. 2015). Knowlton et al. (2004) assessed O_3-related health impacts under climate change scenarios and did sensitivity analysis on modeling assumptions, but their study only discussed health impacts in the New York City. Morita et al. (2014) explored future emission scenarios and their impacts on $PM_{2.5}$-related health outcomes in a global scale, but they did not explore uncertainty due to emission estimates. Madaniyazi at al. (2015a) reviewed studies combining air quality modeling and health impact projections to estimate future mortality and addressed the need to quantify uncertainties within the process.

Most of the studies on air pollution in the Mainland China mainly focused on the distributions and the chemical compositions of the pollutants (eg. He et al. 2001; Zheng et al. 2005; Chan & Yao 2008; Wang et al. 2013; Jie, Ying and Bin 2015; Rohde & Muller 2015). Few studies emphasized epidemiological aspects (eg. Levy & Greco 2007; Public Health and Air Pollution in Asia (PAPA) study, 2008; Cao et al. 2011; Feng et al. 2016). Even fewer studies tried to understand the future health burden that is due to air pollution. Chen et al. (2007) projected PM_{10}-realted mortality in Shanghai in 2020 using four energy scenarios. Pan et al. (2007) also discussed PM_{10}-realted mortality and morbidity outcomes in Beijing in the year 2010, 2020 and 2030 using energy models. Madaniyazi et al (2015b) predicted $PM_{2.5}$-related mortality in East China in 2030 under two emission scenarios. However, all these studies did not include O_3 in their analysis, which is also a public health burden not only in the present year but also in the future. Furthermore, none of these studies tried to assess where the uncertainty lies. Quantifying uncertainties associated with emissions data, C-R functions, and population projections are essential for assessing future air quality management strategies and needs to be explored (Miller et al., 2006).

To fill this gap, our study analyzed both $PM_{2.5}$-and O_3-realted current and future health burden. In addition, we evaluate the sensitivity of each of the different components. Our goal is to estimate whether health outcomes related to $PM_{2.5}$ and O_3 exposure in the Mainland China are sensitive to emission scenarios and C-R functions, and to understand the uncertainty of those inputs in describing future health outcomes. At the same time, when projecting future health outcomes in the Mainland China, it will be important to understand how future pollutant exposures might affect the population in different regions.

The outline of this thesis is as follows: Section 2 explains our study methodology used to evaluate the health impacts and sensitivities. Section 3 describes results. Section 4 discusses the strength and limitations of our study. Finally, Section 5 provides the summary of this study.

Section 2: Methods

For the base year (2008) air quality, we used three emission inventories to simulate $PM_{2.5}$ and O_3 concentrations in January and July (Table2). To project the future air quality (2050), we used four scenarios in the Greenhouse Gas and Air Pollution Interactions and Synergies (GAINS V5a) model. Weather Research and Forecasting (WRF) model coupled with Chemistry (WRF-Chem) was used for all the 14 air quality simulations. We used the 1km x 1km resolution population data in 2008 from Landscan 2008™, and projected 2050 national total population from United Nations' estimates. Providing the population weight to the pollutant concentrations, we measured exposure at the individual level. The change in air pollution levels was quantified by deducting the population-weighted concentration in 2008 from population-weighted concentration in 2050. We later applied the C-R function based on this change to project the mortality and morbidity change in the future. We used an analysis of variance (ANOVA) to quantify the uncertainty, and apportioned the uncertainty to those inputs. Each of the steps is explained in detail below.

2.1 $PM_{2.5}$ and O_3 Concentration Estimation

The three emission inventories we used to quantify base year air quality are: 1) Regional Emission inventory in ASia version 2 (REAS v2, Kurokawa et al., 2013); 2) Multi-resolution Emissions Inventory in China (MEIC, meicmodel.org); and 3) Emissions Database on Global Atmospheric Research version 4.2 (EDGAR v4.2, http://edgar.jrc.ec.europa.eu/). The description of each emission inventory is summarized in Table 2. We used the Weather Research and Forecasting model coupled with Chemistry (WRF-Chem) (Grell et al., 2005) to dynamically simulate base year $PM_{2.5}$ and

O_3 concentrations with the inputs of those emission inventories. For EDGAR specifically, because we lacked the $PM_{2.5}$ estimates, we processed the PM_{10} estimates and converted them into $PM_{2.5}$. We did not simply multiply PM_{10} by 0.6 for the estimation of $PM_{2.5}$ as done by Lei (2013) and others (Levy & Greco 2007) but instead we applied the grid ratio of $PM_{2.5}$ to PM_{10} from REAS simulation result to the EDGAR PM_{10} estimates. This is because we found that the ratio of 0.6 would most likely underestimate $PM_{2.5}$ concentrations for our study.

Figure 3 shows our model domain, which covers countries in East and South Asia with a 20km x 20km resolution. The simulation was conducted for two months: January and July. January is a cold season in China when PM concentrations are the highest (He et al. 2001; Zheng et al. 2005), and July is considered a hot season in China when the O_3 level is the highest (Logan, 1985). Hourly mean $PM_{2.5}$ concentrations (in $\mu g/m^3$) and O_3 mixing ratios (in ppbv) were simulated and summed up for each day. We then averaged the simulation results into monthly mean $PM_{2.5}$ and monthly mean 8-hour average O_3 as a representative of the average exposure in that month in the base year.

For the future projections, we chose the year 2050 as the projection year. There were two reasons for this. First, it is a reasonable year, which is far enough in the future to experience nontrivial emission modification, and is also within a rational range for air quality planning. Second, most of the disagreements of the four Intergovernmental Panel on Climate Change (IPCC) Representative Concentration Pathways (RCPs) scenarios are seen in the year 2050 (Van Vuuren et al. 2007; Clarke et al. 2007; Smith & Wigley, 2006; Wise et al. 2009; Fujino et al. 2006; Hijioka et al. 2008; Riahi et al. 2007)

Appdenix Figure A-1 is a comparison of the emissions from IPCC RCP scenarios, and it is clear that there is a large discrepancy in the emission of organic carbon and black carbon (OC + BC), which are the components of PM, and sulfur dioxide (SO_2) in the year 2050. A large difference is also seen in 2050 in the emissions of carbon monoxide (CO), nitrogen oxides (NOx), and volatile organic compounds (VOCs), which are O_3 precursors.

We did not use RCP scenarios to simulate the 2050 air quality in the Mainland China because they do not include $PM_{2.5}$ emissions estimates. As an alternative, we used the GAINS model to estimate future emissions. We used the following four GAINS scenarios: Assuming current legislation for air pollution (Air), Climate mitigation: limiting average global temperature increase to 2°C (Climate); Short Lived Climate Pollutants mitigation (SLCP); Maximum Technically Feasible Reductions (MTFR) (IIASA, 2006; IEA, 2009).

2.2 Study Population

The population studied in this project is all the residents in the Mainland China. We use the LandScan 2008™ gridded raster data with a 1km x 1km resolution in the year 2008. LandScan 2008™ uses an approach combining Geographic Information System (GIS) with Remote Sensing (RS) for an estimate of population (Dobson et al. 2000). The 1km x 1km raster data was converted to the vector points and aggregated into 20km x 20km gird centroids through ArcGIS 10.3.1 to match the WRF-Chem output and avoid distortion of regridding.

Population projections for 2050 are publicly available on the United Nations Economic and Social Commission for Asia and the Pacific (UN ESCAP) web site (United Nations, 2015). The statistics from the United Nations Department of Economic and Social Affairs

(UN DESA) provide the estimated total population for the Mainland China based on eight scenarios: medium variant (M.V.), high variant (H.V.), low variant (L.V.), constant fertility (C.F.), instant replacement (I.R.), zero migration (Z.M.), constant mortality (C.M.) and no change (N.C.), defined by UN DESA (United Nations, 2015). Since we only have the total population estimate for the year 2050, for each 20km x 20km grid, we multiplied the gridded population in 2008 by the ratio of the total population in 2050 to the total population in the base year 2008 (Figure 1), with the assumption that the proportion of the population in each grid remains constant.

2.3 $PM_{2.5}$ and O_3 Population-Weighted Concentration Estimation

After obtaining monthly-average concentrations from WRF-Chem, we calculated national population-weighted concentrations for each grid centroid using equations X (Eq. 1), combined with the population data, to characterize population exposures.

$$Pop - Weighted_{PM_{2.5}} = \frac{\sum_{i=1}^{n}(PM_i \times Pop_i)}{\sum_{i=1}^{n} Pop_i} \tag{1-a}$$

$$Pop - Weighted_{O_3} = \frac{\sum_{i=1}^{n}(O_{3i} \times Pop_i)}{\sum_{i=1}^{n} Pop_i} \tag{1-b}$$

Where Pop_i is the population for grid i. PM and O_3 are the $PM_{2.5}$ and O_3 concentrations, respectively.

We analyzed regional population-weighted $PM_{2.5}$ and O_3 concentration by aggregating the gridded data to the following seven regions (n in equations 1-a and 1-b): Central, East, North, Northeast, Northwest, South, and Southwest (Figure 2). Regional boundaries of our population data (LandScan 2008™) did not match with the publicly available region and national boundaries such as the Digital Chart of the World (DCW). In order to match the population data, the region shape files were digitalized from the LandScan raster layer using the ArcGIS.

2.4 C-R Function and Health Impact Estimation

The C-R function is a dose-response function quantifying the health outcomes given a change in the pollutant concentrations. To quantitatively analyze health impacts, we applied a log-linear C-R function and relied on the C-R coefficients published by Lei (2013) (Table 3). We used their coefficients to calculate the number of cases avoided or attributed when comparing the future air pollution exposure to the present. A detailed reference is provided in Appendix table A-1.

The health endpoints related to $PM_{2.5}$ pollution include both acute and chronic mortality, and morbidity. The health outcomes for O_3 were limited to acute mortality and morbidity (not include all-cause outpatient visits). Morbidity consists of cardiovascular hospital admissions, respiratory hospital admissions, and all-cause outpatient visits. The health endpoints we analyze are listed in Table 3. The incidence rate for year 2005 was obtained from the Chinese Ministry of Health (MOH) in their statistical yearbook for 2006 (MOH, 2006; Lei 2013), and summarized in Table 4. With the assumption that the incidence rate would not change from 2005, we applied this rate to the future (year 2050) population projections to analyze the baseline incidence. We also held the assumption that the incidence rate is the same for January and July. Since we want to discuss the uncertainty in describing future health impacts, using the same incidence rate can simplify our calculation and reduce noise from other components.

$PM_{2.5}$ and O_3 are the indicators of air pollution in our study, and the C-R function we applied is the same for both $PM_{2.5}$ and O_3 with different coefficients. Lei (2013) used multi-city epidemiological studies on air pollutants in China, and constructed a C-R function, which is applicable for the whole nation. We used their coefficients in health impact analysis, and used 95% confidence interval (CI) from the literature as lower and upper confidence bounds to examine confidence limit.

The projected health outcomes, Y, could be given as:

$$Y = Be^{\beta \Delta x} \tag{2-a}$$

Where B is the baseline incidence when pollutant concentration is 0, β is the C-R coefficient, and Δx is the change in population-weighted air pollutant ($PM_{2.5}$ and O_3) concentrations.

With a log-linear C-R function, we are able to analyze the impact of the change in pollutant concentrations, comparing future (x_1) with base year (x_0), and the corresponding change in health outcomes Δy, with the following C-R function:

$$\Delta \mathrm{y} = \mathrm{y}_{base}\left(e^{\beta \Delta x} - 1\right) \tag{2-b}$$

In Eq (2-b), y_{base} is the baseline incidence in the year 2050 and Δy describes the change in health endpoints using different combinations of present and future emissions scenarios. As a result, our health impact calculation is derived by:

$$\Delta \mathrm{y} = P_{2050} \times r\left(e^{\beta \Delta x} - 1\right) \tag{2-c}$$

Where r is the baseline incidence in Table 4, and P_{2050} and is the population in year 2050. We also calculated health outcomes at a regional level and used regional population-weighted concentration as well as regional population for both 2050 and 2008. In our regional calculation, we used Eq. 2-c and substituted P_{2050} with the population in that specific region.

2.5 Sensitivity analysis

By applying three emission inventories in the present year, four future scenarios in the projected year 2050, one C-R function and eight population projections, we calculated 96 health outcome estimations for the year 2050. Uncertainties exist at each input step. The sensitivity analysis reflects the variations from different factors in health impact estimation (Saltelli at al., 2010). In addition, we also considered the 95% CI of our C-R function, which contributed to more uncertainties in the health estimation.

In order to quantify how much the input factor X_i affects the distribution of health outcome H_i, we used a sensitivity analysis approach using ANOVA decomposition method given the ith input to describe the pattern of the model H=$f(x_1, x_2, \dots x_k)$. The total variance of H can be decomposed to the partial variance that contributed by the total k factors (H|x_1, H|x_2, … H|x_k) and their interactions (H| $x_1, x_2,$ H| x_1, x_3, H| $x_2, x_3,$ … H| $x_1, x_2, x_3 \dots x_k$) (Saltelli at al., 2010).

The decomposition of the total variance, V, is based on:

$$V = V(H|x_1) + V(H|x_2) + \cdots + V(H|x_1, x_2, \dots x_k) \tag{3-a}$$

The associated sensitivity measure Si, which is a first order sensitivity coefficient, is given by:

$$S_i = \frac{V(H|x_i)}{V} \tag{3-b}$$

Si is our sensitivity indices to assess how much variance each input contributed to the total variability. A larger Si indicates larger contribution and vice visa.

Section 3: Results

In this section, we first present model-simulated national air quality in January and July, and compare the results using three different emission inventories in 2008 and four future scenarios in 2050. We then describe the population-weighted concentrations at both national and region levels. We present the national mortality and morbidity of $PM_{2.5}$- and O_3 -related health outcomes by using different emission and population assumptions, followed by a sensitivity analysis to assess the source of the uncertainties.

3.1 National Air quality Characteristics

3.1.1 Base year air quality

Three existing emission inventories were used to simulate the ambient air quality in base year 2008. Figures 4-a and 4-b illustrate the spatial distribution of simulated $PM_{2.5}$ and O_3 burden in January and July in the base year using three different present emission scenarios (REAS, EDGAR, and MEIC). Table 5-a summarizes the mean, median and the standard deviation of the simulation results for both $PM_{2.5}$ and O_3. Standard deviations are 100-120% of the average for $PM_{2.5}$, and 19-25% of the average for O_3, which indicates a high variability for $PM_{2.5}$ concentrations in the nation, compared to the lower variability for O_3. Meteorology, simulated in the air quality model (WRF-Chem) together with transport and chemistry, explains higher $PM_{2.5}$ concentrations in January and increased O_3 concentrations in July. Wet deposition, which occurs less in January, is the major route to remove fine and coarse PM and solar ultraviolet radiation, which peaks in July, is critical for O_3 formation.

Among the simulations using the three different emission inventories, the one using EDGAR (WRF-Chem-EDGAR) produced a 32-40% lower $PM_{2.5}$ in both January and

July, and 3-10% lower O_3 in July compared to simulation results using REAS (WRF-Chem-REAS) and MEIC (WRF-Chem-MEIC) (Table 5-a). This result consents to the previous study, which found a 40-70% higher surface PM_{10}, and a 16–20% higher surface O_3 in North China in July comparing between WRF-Chem-REAS and WRF-Chem-EDGAR in 2007 (Zhong et al. 2015).

We find different spatial patterns of $PM_{2.5}$ and O_3 distribution. In particular, in January, taking WRF-Chem-REAS as an example, the highest $PM_{2.5}$ concentrations were observed in Southwest (207± 25 μg/m^3) and Central China (231 ± 24 μg/m^3), followed by 171 ± 29 μg/m^3 concentrations in the North China. $PM_{2.5}$ concentrations in the rest of the areas were 40% lower compared to the high-pollution areas. This trend assents to the finding of Cao et al. (2012) that mentioned measured winter and summer $PM_{2.5}$ values in 14 Chinese cities located in northern and southern China. They found highest average winter $PM_{2.5}$ in Xi'an (356 μg/m^3), a city in central China, and higher at inland cities compared to the coastal cities. The lowest concentrations among the 14 major cities were observed in Xiamen (74 μg/m^3) in South China. Compared with January, the simulated $PM_{2.5}$ concentrations experienced a pronounced overall decrease (over 50%) in the Mainland China in July. Cao et al. (2004) also found lower concentrations during the summer due to frequent precipitation.

Higher O_3 concentrations (71 ± 9 ppb) were seen in western China, while lower concentrations (51 ± 5 ppb) were found in eastern China in January. Wang et al. (2011) used the model of tropospheric chemistry driven by assimilated meteorological observations from the Global Earth Observing System Chemistry (GEOS-Chem) model to simulate annual mean background surface O_3 concentrations in China and found a similar spatial trend of O_3. In addition, they suggested that the contrast in elevation between West and East China is the major reason of this distribution, because West China has a higher altitude than East China.

Highest O_3 concentrations were found in North China (130 ± 12 ppb), as well as East China (91 ± 11 ppb) for July. As suggested by Wang at al. (2011), a warmer temperature and stronger solar radiation in summer uplift regional O_3 precursors in the summer.

3.1.2 Future year air quality

Projected $PM_{2.5}$ and O_3 distributions are shown in Figures 5-a and 5-b. Projected ambient air pollution in the year 2050 was derived using four different future emission scenarios. Among all the four emission scenarios, simulated pollutant concentrations using the MTFR scenario (WRF-Chem-MTFR) were the lowest both for $PM_{2.5}$ (a mean of 13 ± 17 $\mu g/m^3$ in January) and for O_3 (a mean of 48 ± 10 ppb in July). The low concentrations reflect the reduction in emissions, which led to the decreased $PM_{2.5}$ and O_3 concentrations. The result may be compared to the finding of the Slentø et al. (2009) study. They discussed GAINS emissions in 2020 over Denmark under MTFR scenario, and found that technology adds-ons led to a ~50% emission reductions for NO_x and SO_2, and a 70% reduction for $PM_{2.5}$ emissions compared to their baseline scenario, which assumes maintaining current legislation. They did not discuss the effects on the air pollutants, but it is clear that as a consequence of emissions reduction, $PM_{2.5}$ would be lower compared to the baseline scenario.

WRF-Chem-MTFR estimated an over 80% higher $PM_{2.5}$ concentration in January in East China compared with North China, which was still 40% lower than model-simulated result from Air (WRF-Chem-Air). WRF-Chem-MTFR also estimated 10-16% higher O_3 concentrations in East and North China compared to the Southwest in July.

3.2 Population-weighted concentrations

3.2.1 National Outcomes

The average population-weighted concentrations in China in 2008 were 95 and 47 μg/m^3 per person in January and July, respectively. For O_3 were 39 ppb and 59 ppb per person in January and July, respectively. A recent study (Rohde & Muller, 2015) used data from monitoring sites in China and spatial interpolation methods to conclude an annual mean of 52 μg/m^3 $PM_{2.5}$ population-weighted concentrations. However, they did not consider any seasonal difference. Our result in January is 43 μg/m^3 higher than the annual average and 5 μg/m^3 lower in July compared to the annual mean. Our results demonstrate the need to take inter-annual variability into account.

In 2050, the mean national population-weighted $PM_{2.5}$ concentrations were 49 μg/m^3 per person in January and 31 μg/m^3 per person in July, and 51 ppb per person in January and 51 ppb per person in July for O_3. Figure 6 shows the change in the national population-weighted $PM_{2.5}$ and O_3 concentrations in January and July (future minus base year), with 12 combinations (three exiting emission inventories and four future scenarios). We can see greatly reduced population-weighted $PM_{2.5}$ concentrations (~80 μg/m^3 per person) in January, comparing future to the base year among all 12 combinations, and less than 50% but still decreased $PM_{2.5}$ concentrations in July compared to January. Air-EDGAR, Climate-EDGAR and SLCP-EDGAR predicted slightly increased (up to 10 μg/m^3 per person) population-weighted $PM_{2.5}$ concentrations in July.

The changes in the national population-weighted O_3 concentrations had a different pattern compared to $PM_{2.5}$. Regardless of emissions used in the baseline, WRF-Chem-Air and WRF-Chem-Climate scenarios led to higher population-weighted O_3 concentrations (an up to 15 ppb per person increase) in July, 2050, while WRF-Chem-SLCP and WRF-Chem-MTFR all predicted an up to 13 ppb per person decrease. On the other hand, WRF-Chem-MTFR and WRF-Chem-SLCP showed increased (~15 ppb per person) population-weighted O_3 concentrations in January (Figure 6).

Using different sets of population data did not result in a significant change (mostly less than 0.001 unit per person) in the projected national population-weighted concentrations, both for $PM_{2.5}$ and O_3. The scenario "no change" (constant-fertility and constant-mortality) led to the highest national population-weighted concentrations (see Appendix Table A-3). The increased population-weighted concentrations ranged from 2.27 to 7.71 $\mu g/m^3$ per person for $PM_{2.5}$ and from 5.71 to 8.58 ppb per person for O_3. It is reasonable since "no change" is an extreme assumption, and has the lowest population estimation (Figure 1). The differences in national population-weighted concentrations among the rest of the seven population scenarios were less than 0.001 $\mu g/m^3$ per person for $PM_{2.5}$ and 0.001 ppb per person for O_3. Hence, in the Figure 6, we only show population-weighted concentrations under M.V. population scenario.

3.2.2 Regional Outcomes

To understand how population-weighted exposures vary among regions, we calculated regional specific population-weighted concentrations. Figure 7 shows the population density in China, which illustrates a high population density in East and Central China. Eastern area of the Southwest region also has a high population density due to the big inland cities such as Chongqing. Beijing is in the North region, which brings to the high density of that area. The Tibetan Plateau, which is located in the Southwest, though with scarce population, has the issue of stratospheric intrusion because of its altitude in terms of O_3 pollution.

Regional population-weighted concentrations in 2008 are shown in Figure 8. From the figure, for $PM_{2.5}$, Central and North China were the highest in terms of population-weighted concentrations in January and July, respectively. In January, WRF-Chem-MEIC led to the highest population-weighted concentrations of 166 $\mu g/m^3$ per person for the Central region. In July, WRF-Chem-REAS produced a population-weighted concentration of 86 $\mu g/m^3$ per person in North China.

For O_3, the result varied depending on the emission inventory used. For instance, in January, the highest (50 and 47 ppb per person, respectively) population-weighted concentrations were found in Southwest China from WRF-Chem-REAS and WRF-Chem-MEIC simulations, but in WRF-Chem-EDGAR, it was found in the Nothwest (48 ppb per person). WRF-Chem-REAS and WRF-Chem-EDGAR estimated the lowest population-weighted concentrations in the North China (36 and 39 ppb per person), whereas WRF-Chem-MEIC estimated the lowest in central China (28 ppb per person). Owing to the seasonal difference in the O_3 distribution, North China experienced the highest population-weighted O_3 exposure (68~80 ppb per person) in July. Overall, the difference among the regions was ~40% comparing the highest to the lowest, and it is not as high as it was for $PM_{2.5}$, which was ~70%.

Figure 9 shows the projected regional population-weighted concentrations simulated by four emission scenarios. The highest population-weighted $PM_{2.5}$ concentrations were in

Central China in January and in North China in July, ranging from 44 to 91 μg/m^3 per person and 27 to 65 μg/m^3 per person, respectively. Northeast is predicted to have the lowest population-weighted concentrations in January with an 80% decrease, and south China became the lowest in July with a 25% decrease compared with 2008, regardless of the emission scenarios for the baseline.

We find large discrepancies in 2050 for population-weighted O_3 concentrations among future scenarios. In January, WRF-Chem-Air and WRF-Chem-Climate estimated the highest in the East China (~60 ppb per person), while WRF-Chem-SLCP and WRF-Chem-MTFR predicted the highest in southwest China (~52 ppb per person). High concentrations were found in the Southwest (57 ppb per person), Central (58 ppb per person) and East China (61 ppb per person) under WRF-Chem-Air. WRF-Chem-Climate estimated 56 ppb per person in Central China, 57 ppb per person in North China, and 58 ppb per person in East China. WRF-Chem-SLCP predicted the highest exposure in the Southwest, which is 10% higher than in East China, and WRF-Chem-MTFR showed high population-weighted concentrations in Southwest, Northwest and North China ranging from 51 to 52 ppb per person. In July, the highest population-weighted O_3 concentrations were found in North China, ranging from 67 to 79 ppb per person.

Figure 10 summarizes the regional differences (future minus base year) in population-weighted exposure using various sets of present emission inventories and future scenarios. SLCP-EDGAR leads to a relatively small change (0 to 40 ppb per person in terms of O_3 exposure, and 2 to 20 μg/m^3 per person in terms of $PM_{2.5}$ exposure), and MTFR-MEIC goes through a much larger change (3 to 45 ppb per person in terms of O_3 exposure, and 10 to 120 μg/m^3 per person in terms of $PM_{2.5}$ exposure).

Southwest has the highest reduction (~122 μg/m^3 per person) in $PM_{2.5}$ exposure in January whereas the highest growth of O_3 concentrations (~58 ppb per person) is found in July. This contrast is also found in other studies using different modeling system and emission scenarios. Wang et al. (2013) using Goddard Institute for Space Studies (GISS) Global Climate Model (GCM) simulated 2050 air quality based on the IPCC A1B emission scenario, and found a notable surface O_3 increase in Southwest. They attributed the phenomenon to the increasing anthropogenic emissions from India.

In summary, the national and regional differences in population-weighted concentrations are mainly affected by emission inventories/scenarios, population densities, and seasons. Regions with high population density and high pollutant concentrations such as Central and East China are the places with relatively high population-weighted exposures.

3.3 Health estimates

By applying the C-R function for various health end points, we analyzed national health outcomes (both mortality and morbidity) due to the exposure of $PM_{2.5}$ and O_3. A detailed table with mean national cases attributed and/or avoided with lower and upper limits is presented in the Appendix Table A-6. The 95% CI in the table are based on the published CIs for RR. The reference we use is listed in Appendix Table A-1.

Figure 11 shows the estimated national mortality and morbidity in 2050 by using three different present emission inventories, four future emission scenarios and eight population projections. Compared to the base year in January, an alleviated $PM_{2.5}$ exposure under the four future emission scenarios would avoid ~5,833 to ~31,833 premature deaths from acute effects and ~7,167 to ~154,917 premature deaths from chronic effects under a M.V. population scenario in the Mainland China in 2050 January.

In the same month, a maximum average ~54,667 cardiovascular hospital admission cases can be avoided, as well as a maximum mean ~92,000 respiratory hospital admission cases can be avoided due to the decrease in population-weighted $PM_{2.5}$ exposure, under M.V. population scenario. In the same month, over 800,000 all-causes outpatient visits would be avoided by the improvement of air quality.

In contrast to the large health benefits in January, $PM_{2.5}$ exposure in July in 2050 contributed to more mortalities and morbidities or avoided less cases compared to the year 2008. Compared to the base year, increased $PM_{2.5}$ exposure from WRF-Chem-EDGAR as the base year scenario and WRF-Chem-Air as the future scenario contributed to a mean of ~3,417 premature deaths from acute effects, and ~43,750 premature deaths from chronic effects (with a M.V. population scenario). Health benefits can only be found using WRF-Chem-REAS as the base year scenario and WRF-Chem-MTFR as the future scenario. In terms of the morbidity, most of the scenarios estimated a decrease in morbidity cases, which is shown in Figure 11-a.

Opposite from the $PM_{2.5}$ exposure, O_3 exposures in 2050 compared to the base year predicted an increase in mortality and morbidity. In January, under a M.V. population scenario, WRF-Chem-MEIC combined with WRF-Chem-Air attributed to the highest mean premature deaths estimates (~16,000 cases) from acute effects of O_3 exposure. The lowest was ~2,000 attributed cases from the combination of WRF-Chem-EDGAR and WRF-Chem-MTFR. Mean respiratory admission cases were higher than mean cardiovascular cases, and could contribute up to a mean of ~78,333 and ~92,833 cases for cardiovascular cases and respiratory admission cases, respectively, with a M.V. population scenario.

We found some health benefits in July from O_3 exposure. In terms of premature mortality, WRF-Chem-SLCP and WRF-Chem-MTFR all estimated health benefits, ranging from a mean of ~8,166 and ~1,500, under a M.V. population scenario. The attributed premature deaths could be as high as ~9,917 from WRF-Chem-MEIC and WRF-Chem-Air. The similar phenomenon was seen for morbidity. We could avoid up to a mean of ~37,750 and ~42,333 cases for cardiovascular admission cases and respiratory admission cases, respectively, from WRF-Chem-REAS and WRF-Chem-MTFR, and we also estimated a large increase of ~19,250 cardiovascular admission cases and ~58,250 respiratory admission cases from WRF-Chem-EDGAR and WRF-Chem-Air.

Figure 11 illustrates the differences in mortality and morbidity under eight population projections. Changes in health outcomes using various population projections, though slight, still varied (less than 5% compared with each other).

Because other similar studies used different modeling systems, C-R functions, as well as emission inventories, it is hard to compare our estimates with the published data. Overall, we found more health benefits in January (July) with regard to $PM_{2.5}$ (O_3) exposure, and the difference between January and July is pronounced considering O_3-related health estimations.

3.4 Uncertainty and sensitivity analysis

To quantify $PM_{2.5}$ -and O_3-related mortality in the year 2050, we used three present emission inventories, four future emission scenarios, one C-R function and eight population projections. These are the factors that contribute to the total uncertainty when projecting future health outcomes. The C-R function has its own statistical uncertainty.

We used its 95% CI and thus we derived the lower and upper limits of the mortality and morbidity cases (Appendix Table A-1).

Figure 12 shows the percentage of sensitivity index (Si%) for both mortality and morbidity in January and July, for each species. Uncertainty attributed to the interactions is very small (<1%) and is not shown in the figure. Summary table in Appendix Table A-7 provides a detailed ANOVA result.

Among all the source of variations in projecting future $PM_{2.5}$- and O_3-related health outcomes, $PM_{2.5}$ and O_3 has different distributions of uncertainty. The influence from the sources varies depending on different health endpoints and/or different month.

3.4.1 $PM_{2.5}$ Mortality and Morbidity

Figure 12-a illustrates that present emission inventories were the biggest source of uncertainty for $PM_{2.5}$ in both January and July across both mortality and morbidity. Present emission inventories contribute to be the biggest uncertainty (~74% in January and ~62% in July), followed by future emission scenarios and population projections. The attributed percentage of uncertainty barely changed comparing among both mortality and morbidity (less than 1%). A detailed description is presented below.

In January, present emission inventories account for 74% uncertainty when projecting future acute mortality, and future emission scenarios account for 21% of variability. In terms of chronic mortality, 75% of uncertainty was attributed to the present emission scenarios and 20% uncertainty to the future emission scenarios. The influence from population projection was small, with a 4% contribution for acute and chronic mortality, respectively. In July, for both acute and chronic mortality, present emission inventories contributed 62 and 63% uncertainty in the estimation of $PM_{2.5}$ related health outcomes.

Population projections contributed less compared to January, decreasing to 2% for both acute and chronic mortality.

For morbidity, present emission inventory contributed 74 and 75% uncertainty in the estimation of cardiovascular hospital admission and respiratory hospital admission cases, respectively. Similarly to the national mortality, future emission scenarios are the second significant factor that leads to total uncertainty. The influence from population projections was again 4% for both cardiovascular and respiratory hospital admission. In terms of the outpatient visits, the influence from present emission scenarios slightly decreased by 0.2 to 0.5% compared with other health outcomes.

Similarly to what we concluded in January, present emission inventory is the largest contributor to the total uncertainty, and the future emission scenarios were the second largest factor in July. Compared to January, the uncertainty from present emission scenarios for cardiovascular and respiratory hospital admission cases decreased to 62 and 63%, respectively. We also saw a slight decrease of the attributed uncertainty from population projections (from 4 to 2%). In terms of the outpatient visits, the results are similar.

3.4.2 O_3 Mortality and Morbidity

Figure 11-b shows sensitivity analysis result for O_3-related mortality and morbidity. In contrast to $PM_{2.5}$, the largest uncertainty is from the future emission scenarios (53% in January and 79% in July), and the change in sensitivity index between different months is bigger compared to $PM_{2.5}$. Population projections contributed to 7% of the total availability both in January and July. A detailed description is given below.

The future emission scenarios accounted for 53% and 79% of uncertainty when projecting national acute mortality in January and July, respectively, with the influence from present emission scenarios decreasing from 39% in January to 13% in July. Population projections still have a relatively smaller contribution to the total variability, with a proportion of 8% in January and 7% in July.

Similarly to the national mortality, the future emission scenarios have a bigger impact on the total uncertainty than present emission scenarios when projecting national morbidity. Future emission scenarios contributed 53% of uncertainty for both cardiovascular hospital admission and respiratory hospital admission cases.

In July, the uncertainty from future emission scenarios increased 27% for cardiovascular hospital admission and respiratory hospital admission cases, respectively. For both January and July, population projection contributed 8% and 7% uncertainties for both cardiovascular hospital admission and respiratory hospital admission cases.

Section 4: Discussions

We found a reduction in mortality and morbidity in 2050 due to decreased national population-weighted $PM_{2.5}$ concentrations in winter and slightly-reduced O_3 concentrations in summer, compared to 2008. The increase of O_3 in January 2050 contributed to the excess mortality and morbidity. Health effects induced by $PM_{2.5}$ had a larger variation compared to O_3 mainly due to the significant decrease in population-weighted concentrations in 2050, and a higher coefficient in the C-R function for $PM_{2.5}$. The greatest health benefits were found using the MTFR scenario regardless of what emission inventories were used to characterize present air quality. It avoided up to 30 times the cases than the worst scenario for $PM_{2.5}$ in January, and avoided two to three times the cases for O_3 in July compared with the worst scenario. We found the largest burden of disease under the Air scenario, assuming the implementation of all currently agreed air pollution policies, regardless of which base year emissions were chosen. The result that MTFR is the most benefit future scenario and Air is the worst is consistent with the reduction rate of air pollutant species from a recent study comparing GAINS' four scenarios globally (Pietikäinen et al., 2015).

From the sensitivity analysis, we found that the major source of uncertainty came from emission scenarios. Specifically, present emissions have the greatest uncertainty (up to 74%) when projecting $PM_{2.5}$-related health outcomes in January; future emission scenarios contribute the most (up to 79%) to the uncertainty in O_3-related health outcome estimations in July. The large uncertainty we found suggests that we cannot rely on a single emission inventory or future emission scenario when projecting air pollution-related health estimates. Similar studies, Kim et al. (2015) and Post et al. (2013)

discussed O_3-related health estimates in the U.S. and found different source of uncertainty. Post et al. (2013) attributed the largest uncertainty to the model choice since they focused on climate-related consequences instead of emissions levels as we did. Kim et al. (2015) attributed the highest uncertainty to RCP scenarios in projecting future O_3 levels, but they did not discuss the current emission scenarios.

Similar studies that used this approach to assess the potential health outcomes of $PM_{2.5}$ and O_3 in China were only conducted at the provincial or city levels (for example, Madaniyazi et. al, 2015b in East region; Jie et al. 2015 in North China), while we addressed this issue on national and regional levels. Although the previous city-level studies described possible uncertainties of their study, they did not include those underlying sources of uncertainty when conducting the analysis. Our research considered potential variability in projecting health issues and utilized variance decomposition method to source the uncertainty. We highlight the impact of current and future emissions on population health. Further, we showed the spatial variability of population-weighted concentrations among regions within China. The result emphasizes the need of region-specific health assessments.

The major strength of our research is our study scale with a relatively fine data resolution. We projected the national variability of $PM_{2.5}$- and O_3-related mortality and morbidity under several possible sources of uncertainty with a 20km x 20km resolution, which enabled us to estimate both regional and national impacts. To the best of our knowledge, this is the first study to project the $PM_{2.5}$- and O_3-related health outcomes at the national level in China while comparing two specific months and analyzing the proportion of uncertainty to each input (present emissions, future emission scenarios, and population projections). In addition, this is one of the few studies comparing the impact of different existing emission inventories on health outcome estimations in China. In terms of applying GAINS emission inventory in China, studies have normally emphasized technology assessment, such as the one by Dong et al. (2015). Fewer studies aimed at projecting health aspects in China. Furthermore, our work highlights the need to handle various uncertainties, including better constraining current emissions.

There are several limitations in our study. First, in our future simulation, we do not take climate change into consideration. As a result, our sensitivity analysis did not address the uncertainty from changing climate. This was because we were interested in focusing on comparing emission scenarios and addressing their uncertainty before introducing even larger uncertainty. Second, we assumed that the incidence rate of both $PM_{2.5}$- and O_3-related mortality and morbidity is the same in 2050 as our base year and the target population is exposed to a single pollutant. We also did not include age-specific analysis. Those assumptions may underestimate the mortality and morbidity rates for future populations. Nevertheless, those limitations are constrained by the C-R function and data availability for China. Despite the limitation in the health estimation in our study, we have emphasized the change in the health outcomes compared to the base year instead of the number of cases estimated. The uncertainty that resulted from these assumptions would not affect the overall sensitivity analysis.

Section 5: Conclusions and Recommendations

We find that present emission inventories and future emission scenarios are the major source of uncertainty in calculating health outcomes in the Mainland China. The origin and the magnitude of emissions have a great impact on premature mortality and morbidity calculation. Our results illustrate that constraining emissions in the present is essential for quantifying health benefits.

Reference

Bravo, M. A., Fuentes, M., Zhang, Y., Burr, M. J., & Bell, M. L. (2012). Comparison of exposure estimation methods for air pollutants: ambient monitoring data and regional air quality simulation. *Environmental research*, 116, 1-10. doi:10.1016/j.envres.2012.04.008.

Cao, J. J., Lee, S. C., Ho, K. F., Zou, S. C., Fung, K., Li, Y., ... & Chow, J. C. (2004). Spatial and seasonal variations of atmospheric organic carbon and elemental carbon in Pearl River Delta Region, China. *Atmospheric Environment*, *38*(27), 4447-4456. doi:10.1016/j.atmosenv.2004.05.016.

Cao, J. J., Shen, Z. X., Chow, J. C., Watson, J. G., Lee, S. C., Tie, X. X., ... & Han, Y. M. (2012). Winter and summer PM2. 5 chemical compositions in fourteen Chinese cities. *Journal of the Air & Waste Management Association*, *62*(10), 1214-1226. DOI:10.1080/10962247.2012.701193.

Cao, J., Yang, C., Li, J., Chen, R., Chen, B., Gu, D., & Kan, H. (2011). Association between long-term exposure to outdoor air pollution and mortality in China: a cohort study. *Journal of Hazardous Materials*, 186(2), 1594-1600. doi:10.1016/j.jhazmat.2010.12.036.

Chan, C. K., & Yao, X. (2008). Air pollution in mega cities in China. *Atmospheric environment*, 42(1), 1-42. doi:10.1016/j.atmosenv.2007.09.003.

Chen, C., Chen, B., Wang, B., Huang, C., Zhao, J., Dai, Y., & Kan, H. (2007). Low-carbon energy policy and ambient air pollution in Shanghai, China: a health-based economic assessment. *Science of the Total Environment*, 373(1), 13-21.

Chinadaily. 2016. China's National Ambient Air Quality Situation: A Report from the MEP (in Chinese) Available: http://world.chinadaily.com.cn/2016-02/04/content_23392866.htm [accessed 24 March 2016]

Clarke, L., J. Edmonds, H. Jacoby, H. Pitcher, J. Reilly, R. Richels, 2007. Scenarios of Greenhouse Gas Emissions and Atmospheric Concentrations. Sub-report 2.1A of Synthesis and Assessment Product 2.1 by the U.S. Climate Change Science Program and the Subcommittee on Global Change Research. Department of Energy, Office of Biological & Environmental Research, Washington, 7 DC., USA, 154 pp.

Correia, A. W., Pope III, C. A., Dockery, D. W., Wang, Y., Ezzati, M., & Dominici, F. (2013). The effect of air pollution control on life expectancy in the United States: an analysis of 545 US counties for the period 2000 to 2007. *Epidemiology (Cambridge, Mass.)*, 24(1), 23. doi: 10.1097/EDE.0b013e3182770237.

Daniels, M. J., Dominici, F., Samet, J. M., & Zeger, S. L. (2000). Estimating particulate matter-mortality dose-response curves and threshold levels: an analysis of daily time-series for the 20 largest US cities. *American journal of epidemiology*, 152(5), 397-406. doi: 10.1093/aje/152.5.397.

Delfino, R. J., Murphy-Moulton, A. M., & Becklake, M. R. (1998). Emergency room visits for respiratory illnesses among the elderly in Montreal: association with low level ozone exposure. *Environmental Research*, 76(2), 67-77. doi:10.1006/enrs.1997.3794.

Dobson, J. E., Bright, E. A., Coleman, P. R., Durfee, R. C., & Worley, B. A. (2000). LandScan: a global population database for estimating populations at risk. *Photogrammetric engineering and remote sensing*, *66*(7), 849-857.

Dockery, D. W., Pope, C. A., Xu, X., Spengler, J. D., Ware, J. H., Fay, M. E., ... & Speizer, F. E. (1993). An association between air pollution and mortality in six US cities. *New England journal of medicine*, 329(24), 1753-1759. DOI: 10.1056/NEJM199312093292401.

Dong, L., Dong, H., Fujita, T., Geng, Y., & Fujii, M. (2015). Cost-effectiveness analysis of China's Sulfur dioxide control strategy at the regional level: regional disparity, inequity and future challenges. *Journal of Cleaner Production*, *90*, 345-359. doi:10.1016/j.jclepro.2014.10.101.

Feng, C., Li, J., Sun, W., Zhang, Y., & Wang, Q. (2016). Impact of ambient fine particulate matter (PM 2.5) exposure on the risk of influenza-like-illness: a time-series analysis in Beijing, China. *Environmental Health*, 15(1), 1. DOI: 10.1186/s12940-016-0115-2.

Franklin, M., Zeka, A., & Schwartz, J. (2007). Association between PM2. 5 and all-cause and specific-cause mortality in 27 US communities. *Journal of Exposure Science and Environmental Epidemiology*, 17(3), 279-287. doi:10.1038/sj.jes.7500530.

Fujino, J., R. Nair, M. Kainuma, T. Masui, Y. Matsuoka, 2006. Multi-gas mitigation analysis on stabilization scenarios using AIM global model. Multigas Mitigation and Climate Policy. *The Energy Journal Special Issue*, 27, 343-353.

Geels, C., Andersson, C., Hänninen, O., Lansø, A. S., Schwarze, P. E., Skjøth, C. A., & Brandt, J. (2015). Future Premature Mortality Due to O3, Secondary Inorganic Aerosols and Primary PM in Europe—Sensitivity to Changes in Climate, Anthropogenic Emissions, Population and Building Stock. *International journal of environmental research and public health*, *12*(3), 2837-2869. doi:10.3390/ijerph120302837.

Green Peace. 2015. A Summary of the 2015 Annual $PM_{2.5}$ City Rankings. Available: http://www.greenpeace.org/eastasia/Global/eastasia/publications/reports/climate-energy/2015/GPEA%202015%20City%20Rankings_briefing_int.pdf[accessed 12 February 2016]

Gschwind, B., Lefevre, M., Blanc, I., Ranchin, T., Wyrwa, A., Drebszok, K., ... & Fuss, S. (2015). Including the temporal change in PM 2.5 concentration in the assessment of human health impact: Illustration with renewable energy scenarios to 2050. *Environmental Impact Assessment Review*, *52*, 62-68. doi:10.1016/j.eiar.2014.09.003.

Hajat, A., Allison, M., Diez-Roux, A. V., Jenny, N. S., Jorgensen, N. W., Szpiro, A. A., ... & Kaufman, J. D. (2015). Long-term exposure to air pollution and markers of inflammation, coagulation, and endothelial activation: a repeat-measures analysis in the Multi-Ethnic Study of Atherosclerosis (MESA). *Epidemiology*, 26(3), 310-320. doi: 10.1097/EDE.0000000000000267.

Halonen, J. I., Lanki, T., Tiittanen, P., Niemi, J. V., Loh, M., & Pekkanen, J. (2009). Ozone and cause-specific cardiorespiratory morbidity and mortality. *Journal of epidemiology and community healt*h, jech-2009. doi:10.1136/jech.2009.087106.

He, K., Yang, F., Ma, Y., Zhang, Q., Yao, X., Chan, C. K., ... & Mulawa, P. (2001). The characteristics of PM 2.5 in Beijing, China. *Atmospheric Environment*, 35(29), 4959-4970. doi:10.1016/S1352-2310(01)00301-6.

Hijioka, Y., Y. Matsuoka, H. Nishimoto, M. Masui, and M. Kainuma, 2008. Global GHG emissions scenarios under GHG concentration stabilization targets. *Journal of Global Environmental Engineering* 13, 97-108.

Hoek, G., Krishnan, R. M., Beelen, R., Peters, A., Ostro, B., Brunekreef, B., & Kaufman, J. D. (2013). Long-term air pollution exposure and cardio-respiratory mortality: a review. *Environ Health*, 12(1), 43.

Huang, R. J., Zhang, Y., Bozzetti, C., Ho, K. F., Cao, J. J., Han, Y., ... & Zotter, P. (2014). High secondary aerosol contribution to particulate pollution during haze events in China. *Nature*, 514(7521), 218-222. doi:10.1038/nature13774.

IEA (International Energy Agency). 2009. World Energy Outlook:2009. Available: https://www.iea.org/textbase/npsum/weo2009sum.pdf [accessed 10 April 2016]

IIASA (International Institute for Applied Systems Analysis). 2016. Global emission fields of air pollutants and GHGs. Available: http://www.iiasa.ac.at/web/home/research/researchPrograms/air/Global_emissions.html [accessed 10 April 2016]

Jie, W., Ying, X., & Bing, Z. (2015). Projection of PM2. 5 and ozone concentration changes over the Jing-Jin-Ji region in China. *Atmospheric and Oceanic Science Letters*, *8*(3), 143-146. DOI:10.3878/AOSL20140102.

Kappos, A. D., Bruckmann, P., Eikmann, T., Englert, N., Heinrich, U., Höppe, P., ... & Rombout, P. (2004). Health effects of particles in ambient air. *International Journal of Hygiene and Environmental Health*, 207(4), 399-407. doi:10.1078/1438-4639-00306.

Kim, Y. M., Zhou, Y., Gao, Y., Fu, J. S., Johnson, B. A., Huang, C., & Liu, Y. (2015). Spatially resolved estimation of ozone-related mortality in the United States under two representative concentration pathways (RCPs) and their uncertainty. *Climatic change*, *128*(1-2), 71-84. doi:10.1007/s10584-014-1290-1.

Knowlton, K., Rosenthal, J. E., Hogrefe, C., Lynn, B., Gaffin, S., Goldberg, R., ... & Kinney, P. L. (2004). Assessing ozone-related health impacts under a changing climate. *Environmental Health Perspectives*, 112(15), 1557-1563.

Lei. Y. (2013). Benefits to Human Health and Agricultural Productivity of Reduced Air Pollution. In Nielsen, C. P., & Ho, M. S. (Eds.). *Clearer Skies over China* (291-328). Cambridge, US: The MIT Press.

Lelieveld, J., Evans, J. S., Fnais, M., Giannadaki, D., & Pozzer, A. (2015). The contribution of outdoor air pollution sources to premature mortality on a global scale. *Nature*, *525*(7569), 367-371. doi:10.1038/nature15371.

Levy, J. I., & Greco, S. L. (2007). Estimating health effects of air pollution in China: an introduction to intake fraction and the epidemiology. *Clearing the Air: The Health and Economic Damages of Air Pollution in China (Ho MS, Nielsen CP, eds). Cambridge, MA: MIT Press*, 115-142.

Levy, J. I., Chemerynski, S. M., & Sarnat, J. A. (2005). Ozone exposure and mortality: an empiric bayes metaregression analysis. *Epidemiology*, 16(4), 458-468. doi: 10.1097/01.ede.0000165820.08301.b3.

Lippmann, M., Ito, K., Nadas, A., & Burnett, R. T. (2000). Association of particulate matter components with daily mortality and morbidity in urban populations. *Research report (Health Effects Institute)*, (95), 5-72.

Logan, J. A. (1985). Tropospheric ozone: Seasonal behavior, trends, and anthropogenic influence. Journal of Geophysical Research: *Atmospheres*,90(D6), 10463-10482.

Madaniyazi, L., Guo, Y., Yu, W., & Tong, S. (2015a). Projecting future air pollution-related mortality under a changing climate: progress, uncertainties and research needs. *Environment international*, 75, 21-32. doi:10.1016/j.envint.2014.10.018.

Madaniyazi, L., Nagashima, T., Guo, Y., Yu, W., & Tong, S. (2015b). Projecting Fine Particulate Matter-Related Mortality in East China. *Environmental science & technology*, *49*(18), 11141-11150. DOI: 10.1021/acs.est.5b01478.

Markakis, K., Valari, M., Perrussel, O., Sanchez, O., & Honore, C. (2015). Climate-forced air-quality modeling at the urban scale: sensitivity to model resolution, emissions and meteorology. *Atmospheric Chemistry and Physics*, *15*(13), 7703-7723. doi:10.5194/acp-15-7703-2015.

MEP (The Ministry of Environmental Protection of the People's Republic of China). 1996. The National Ambient Air Quality Standards (GB 3095-1996). Available: http://www.mep.gov.cn/image20010518/5298.pdf [accessed 12 February 2015]

MEP (The Ministry of Environmental Protection of the People's Republic of China). 2012. The National Ambient Air Quality Standards (GB 3095-2012). Available: http://kjs.mep.gov.cn/hjbhbz/bzwb/dqhjbh/dqhjzlbz/201203/W020120410330232398521.pdf [accessed 12 February 2016]

MEP (The Ministry of Environmental Protection of the People's Republic of China). 2016. Air Quality Daily [dataset]. Available: http://datacenter.mep.gov.cn/report/air_daily/air_dairy_en.jsp [accessed 04 March 2016]

Morita, H., Yang, S., Unger, N., & Kinney, P. L. (2014). Global Health Impacts of Future Aviation Emissions Under Alternative Control Scenarios. *Environmental science & technology*, *48*(24), 14659-14667. DOI: 10.1021/es5055379.

Özkaynak, H., Baxter, L. K., Dionisio, K. L., & Burke, J. (2013). Air pollution exposure prediction approaches used in air pollution epidemiology studies. *Journal of Exposure Science and Environmental Epidemiology*, 23(6), 566-572. doi:10.1038/jes.2013.15.

Pan, X., Yue, W., He, K., & Tong, S. (2007). Health benefit evaluation of the energy use scenarios in Beijing, China. *Science of the total environment*, 374(2), 242-251. doi:10.1016/j.scitotenv.2007.01.005.

Patz, J. A., Campbell-Lendrum, D., Holloway, T., & Foley, J. A. (2005). Impact of regional climate change on human health. *Nature*, 438(7066), 310-317.DOI: 10.1038/nature04188.

Pietikäinen, J. P., Kupiainen, K., Klimont, Z., Makkonen, R., Korhonen, H., Karinkanta, R., ... & Kerminen, V. M. (2015). Impacts of emission reductions on aerosol radiative effects. *Atmospheric Chemistry and Physics*, *15*(10), 5501-5519. doi:10.5194/acp-15-5501-2015.

Pope III, C. A., Burnett, R. T., Thun, M. J., Calle, E. E., Krewski, D., Ito, K., & Thurston, G. D. (2002). Lung cancer, cardiopulmonary mortality, and long-term exposure to fine particulate air pollution. *Jama*, *287*(9), 1132-1141. doi:10.1001/jama.287.9.1132.

Post, E. S., Grambsch, A., Weaver, C., Morefield, P., Huang, J., Leung, L. Y., ... & Mahoney, H. (2012). Variation in estimated ozone-related health impacts of climate change due to modeling choices and assumptions.*Environmental health perspectives*, *120*(11), 1559. doi: 10.1289/ehp.1104271.

Riahi, K. Gruebler, A. and Nakicenovic N.: 2007. Scenarios of long-term socio-economic and environmental development under climate stabilization. *Technological Forecasting and Social Change* 74, 7, 887-935. doi:10.1016/j.techfore.2006.05.026

Rohde, R. A., & Muller, R. A. (2015). Air pollution in China: Mapping of concentrations and sources. *PloS one*, *10*(8), e0135749.

Saikawa, E., Young, C. L., Kim, H., Kurokawa, J. I., Zhao, Y., Janssens-Maenhout, G. G. A., ... & Ohara, T. (2014, December). Comparison of Emissions Inventories of Anthropogenic Air Pollutants in Asia. In *AGU Fall Meeting Abstracts* (Vol. 1, p. 06).

Saltelli, A., Annoni, P., Azzini, I., Campolongo, F., Ratto, M., & Tarantola, S. (2010). Variance based sensitivity analysis of model output. Design and estimator for the total sensitivity index. *Computer Physics Communications*,*181*(2), 259-270. doi:10.1016/j.cpc.2009.09.018.

Samet, J. M., Zeger, S. L., Dominici, F., Curriero, F., Coursac, I., Dockery, D. W., ... & Zanobetti, A. (2000). The national morbidity, mortality, and air pollution study. Part II: morbidity and mortality from air pollution in the United States Res Rep Health Eff Inst, 94(pt 2), 5-79.

Seaman, N. L. (2000). Meteorological modeling for air-quality assessments. *Atmospheric environment*, 34(12), 2231-2259. doi:10.1016/S1352-2310(99)00466-5.

Slentø, E., Nielsen, O. K., Hoffmann, L., Winther, M., Fauser, P., Mikkelsen, M. H., & Gyldenkærne, S. (2009). *NEC-2020 emission reduction scenarios: Assessment of intermediary GAINS emission reduction scenarios for Denmark aiming at the upcoming 2020 National Emission Ceilings EU directive*. National Environmental Research Institute, Aarhus University.

Smith, S.J. and T.M.L. Wigley, 2006. Multi-Gas Forcing Stabilization with the MiniCAM. *Energy Journal* (Special Issue #3). 27. 373-391.

Strak, M., Janssen, N. A., Godri, K. J., Gosens, I., Mudway, I. S., Cassee, F. R., ... & Steenhof, M. (2012). Respiratory health effects of airborne particulate matter: the role of particle size, composition, and oxidative potential-the RAPTES project. *Environmental health perspectives*, 120(8), 1183. doi: 10.1289/ehp.1104389.

Tecer, L. H., Alagha, O., Karaca, F., Tuncel, G., & Eldes, N. (2008). Particulate matter (PM2. 5, PM10-2.5, and PM10) and children's hospital admissions for asthma and respiratory diseases: A bidirectional case-crossover study. *Journal of Toxicology and Environmental Health, Part A*, 71(8), 512-520. DOI:10.1080/15287390801907459.

The World Bank. 2016. Population ranking: Population 2014. Available: http://data.worldbank.org/data-catalog/Population-ranking-table [accessed 17 April 2016]

Tonne, C., Yanosky, J. D., Beevers, S., Wilkinson, P., & Kelly, F. J. (2012). PM mass concentration and PM oxidative potential in relation to carotid intima-media thickness. *Epidemiology*, 23(3), 486-494. doi: 10.1097/EDE.0b013e31824e613e.

van Vuuren, D., M. den Elzen, P. Lucas, B. Eickhout, B. Strengers, B. van Ruijven, S. Wonink, R. van Houdt, 2007. Stabilizing greenhouse gas concentrations at low levels: an assessment of reduction strategies and costs. *Climatic Change*, doi:10.1007/s/10584-006-9172-9.

Wang, Y., Shen, L., Wu, S., Mickley, L., He, J., & Hao, J. (2013). Sensitivity of surface ozone over China to 2000–2050 global changes of climate and emissions. *Atmospheric Environment*, *75*, 374-382. doi:10.1016/j.atmosenv.2013.04.045.

Wang, Y., Zhang, Y., Hao, J., and Luo, M (2011): Seasonal and spatial variability of surface ozone over China: contributions from background and domestic pollution, *Atmos. Chem. Phys*., 11, 3511-3525, doi:10.5194/acp-11-3511-2011

Weichenthal, S. A., Godri-Pollitt, K., & Villeneuve, P. J. (2013). PM2. 5, oxidant defence and cardiorespiratory health: a review. *Environ Health*, 12(40), 10-1186. doi: 10.1186/1476-069X-12-40.

WHO (World Health Organization). 2014. Ambient (outdoor) air quality and health. Available: http://www.who.int/mediacentre/factsheets/fs313/en/ [accessed 17 April 2016]

Wise, MA, KV Calvin, AM Thomson, LE Clarke, B Bond-Lamberty, RD Sands, SJ Smith, AC Janetos, JA Edmonds. 2009. Implications of Limiting CO2 Concentrations for Land Use and Energy. *Science*. 324:1183-1186. May 29, 2009. DOI: 10.1126/science.1168475.

Wong, C. M., Vichit-Vadakan, N., Kan, H., & Qian, Z. (2008). Public Health and Air Pollution in Asia (PAPA): a multicity study of short-term effects of air pollution on mortality. *Environmental Health Perspectives*, *116*(9), 1195. doi: 10.1289/ehp.11257.

Wong, T. W., Lau, T. S., Yu, T. S., Neller, A., Wong, S. L., Tam, W., & Pang, S. W. (1999). Air pollution and hospital admissions for respiratory and cardiovascular diseases in Hong Kong. *Occupational and environmental medicine*, *56*(10), 679-683.

Xu, X., Li, B., & Huang, H. (1995). Air pollution and unscheduled hospital outpatient and emergency room visits. *Environmental Health Perspectives*,*103*(3), 286.

You, M. (2014). Addition of PM 2.5 into the National Ambient Air Quality Standards of China and the Contribution to Air Pollution Control: The Case Study of Wuhan, China. *The Scientific World Journal*, 2014. doi: 10.1155/2014/768405.

Zhang, J., Ouyang, Z., Miao, H., & Wang, X. (2011). Ambient air quality trends and driving factor analysis in Beijing, 1983–2007. *Journal of Environmental Sciences*, 23(12), 2019-2028. doi:10.1016/S1001-0742(10)60667-5.

Zheng, M., Salmon, L. G., Schauer, J. J., Zeng, L., Kiang, C. S., Zhang, Y., & Cass, G. R. (2005). Seasonal trends in PM2. 5 source contributions in Beijing, China. *Atmospheric Environment*, 39(22), 3967-3976. doi:10.1016/j.atmosenv.2005.03.036.

Zhong, M., Saikawa, E., Liu, Y., Naik, V., Horowitz, L. W., Takigawa, M., ... & Stone, E. A. (2015). Air Quality Modeling with WRF-Chem v3. 5 in East and South Asia: sensitivity to emissions and evaluation of simulated air quality. *Geoscientific Model Development Discussions*, *8*(10), 9373-9413. doi:10.5194/gmdd-8-9373-2015

Tables & Figures

Table 1. $PM_{2.5}$ and O_3 guidelines by Chinese NAAQS and WHO, and a comparison with the U.S. standard.

	NAAQS Limits (GB 3095-1996)	NAAQS Limits (GB 3095-2012)	WHO Guidelines	U.S. NAAQS (40 CFR part 50) Limits
$PM_{2.5}$ annual mean ($\mu g/m^3$)	NA	35	10	12
$PM_{2.5}$ 24-hour mean($\mu g/m^3$)	NA	75	25	35
O_3 8-hour mean ($\mu g/m^3$)	NA	160	100	140
O_3 Hourly ($\mu g/m^3$)	120	200	NA	235

Table 2. Summary of the emission inventories and a model used in air quality simulation

Emission Inventory/ Model	Area	Year	Spatial Resolution	Reference
REAS	Asia	2000-2008	0.25° x 0.25°	Kurokawa et al., 2013
MEIC	China	1990-2010	User defined	meicmodel.org
EDGAR	Global	1970-2008	0.1° x 0.1°	http://edgar.jrc.ec.europa.eu
GAINS	Global	1990-2050	0.5° x 0.5°	http://gains.iiasa.ac.at/models/index.html

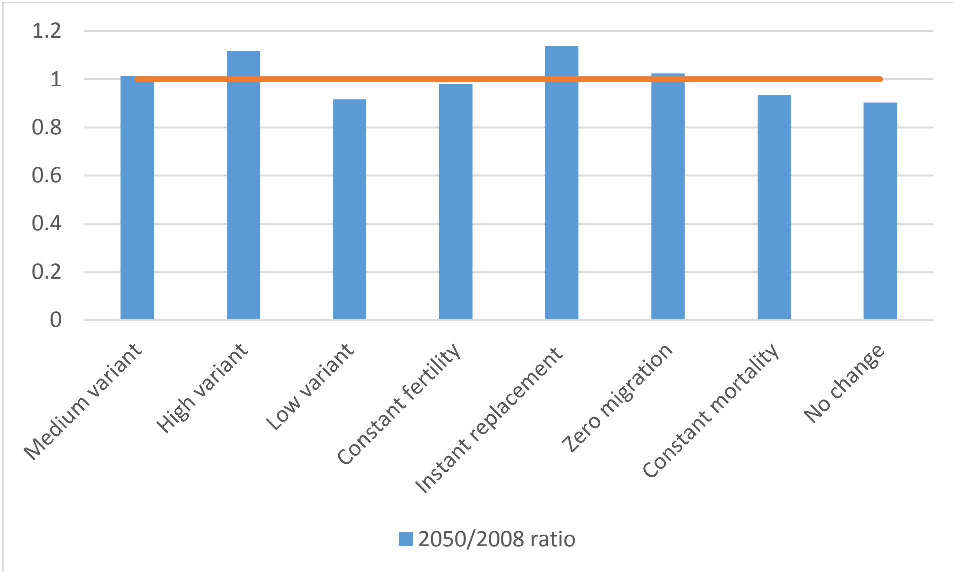

Figure 1. Summary of the ratio of 2050 total population in each scenario to 2008 total population (population number). Orange line equals one.

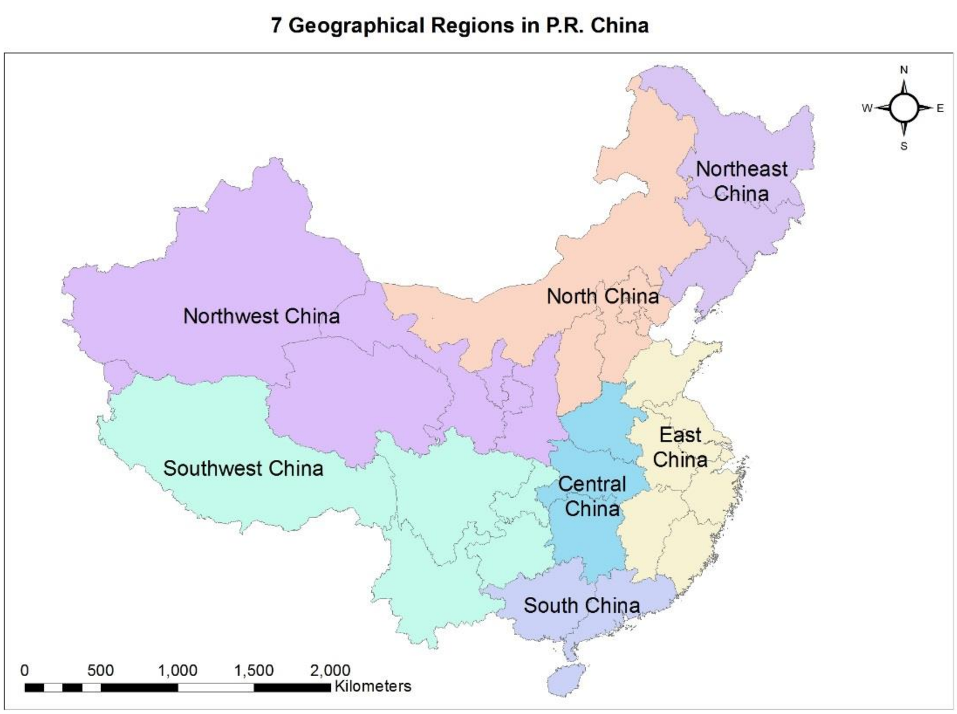

Figure 2. Geographical regions of the Mainland China in our study

Figure 3. Model domain of the WRF-Chem simulation using a Lambert Conformal Conic projection.

Table 3. Summary of C-R function Coefficients (β)

Health Endpoints	β for $PM_{2.5}$ β (upper, lower of 95% CI)	β for O_3 β (upper, lower of 95% CI)
Acute mortality	0.000646 (0.000499,0.00698)	0.001161 (0.0004873, 0.001796)
Chronic mortality	0.003922 (0.000995, 0.007696)	
Hospital admissions, cardiovascular	0.000997 (0.000333,0.001823)	0.004844 (0.001871, 0.007796)
Hospital admissions, respiratory	0.002646 (0.001658,0.003627)	0.008161 (0.005585, 0.010724)
Outpatient visits, all causes	0.000391 (0.000242,0.0005188)	

Abbreviation: CI: Confidence Interval

Table 4. Summary of incidence rates

Health Outcomes	Incidence Rate r*
All-cause mortality	0.0055
Hospital admissions, cardiovascular	0.0062
Hospital admissions, respiratory	0.0042
Outpatient visits, all causes	3.4788

*rates are cases per person per year

Table 5-a. Summary statistics of monthly mean $PM_{2.5}$ and O_3 concentrations in China from air quality simulations using three different present emission inventories in 2008. Numbers are rounded to the nearest hundredth

Present Emission Inventory (Month)	$PM_{2.5}$ (μg/m^3)				O_3 (ppbv)			
	Mean	Min.	Max.	Sd.	Mean	Min.	Max.	Sd.
REAS (Jan.)	42.12	1.24	293.50	50.85	51.61	4.77	71.26	10.46
MEIC (Jan.)	44.25	1.16	299.60	54.89	49.53	4.86	71.31	12.34
EDGAR (Jan.)	27.22	1.05	386.40	32.01	52.47	4.73	70.89	8.95
REAS (July)	21.64	1.04	321.00	26.91	57.58	3.65	130.10	10.48
MEIC (July)	19.95	0.88	150.30	24.48	53.39	9.28	86.02	9.32
EDAGR (July)	13.31	1.00	276.70	14.09	51.85	8.33	111.00	9.52

Table 5-b. Summary statistics of monthly mean $PM_{2.5}$ and O_3 concentrations in China from air quality simulations using four different future emission scenarios in 2050. Numbers are rounded to the nearest hundredth

Future Emission scenario (Month)	$PM_{2.5}$ (μg/m^3)				O_3 (ppbv)			
	Mean	Min.	Max.	Sd.	Mean	Min.	Max.	Sd.
Air (Jan.)	25.38	1.43	240.60	30.21	56.67	37.89	81.71	6.85
Climate (Jan.)	20.46	1.01	229.70	25.96	55.58	34.09	73.35	6.84
SLCP (Jan.)	20.46	1.07	221.70	25.21	52.87	28.88	70.85	8.06
MTFR (Jan.)	12.99	0.57	206.60	17.20	52.09	26.92	70.18	8.48
Air (July)	15.87	1.22	129.30	18.93	56.92	25.63	138.20	12.50
Climate (July)	12.38	0.94	117.10	15.07	53.77	21.62	116.80	11.66
SLCP (July)	13.12	1.13	110.80	15.69	49.94	19.15	91.75	9.90
MTFR (July)	7.21	0.48	124.50	8.70	47.81	16.88	94.30	9.82

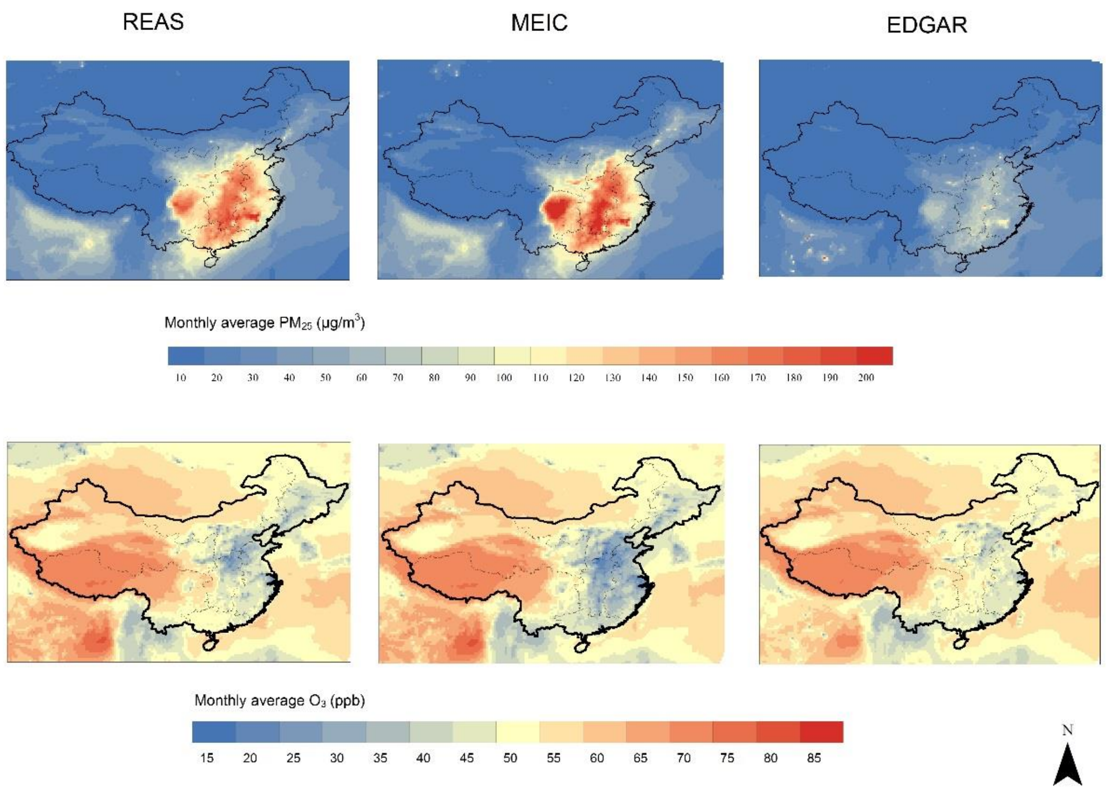

Figure 4-a. Spatial distribution of $PM_{2.5}$ and O_3 concentrations in January, 2008. Units for $PM_{2.5}$ and O_3 are $\mu g/m^3$ and ppb, respectively.

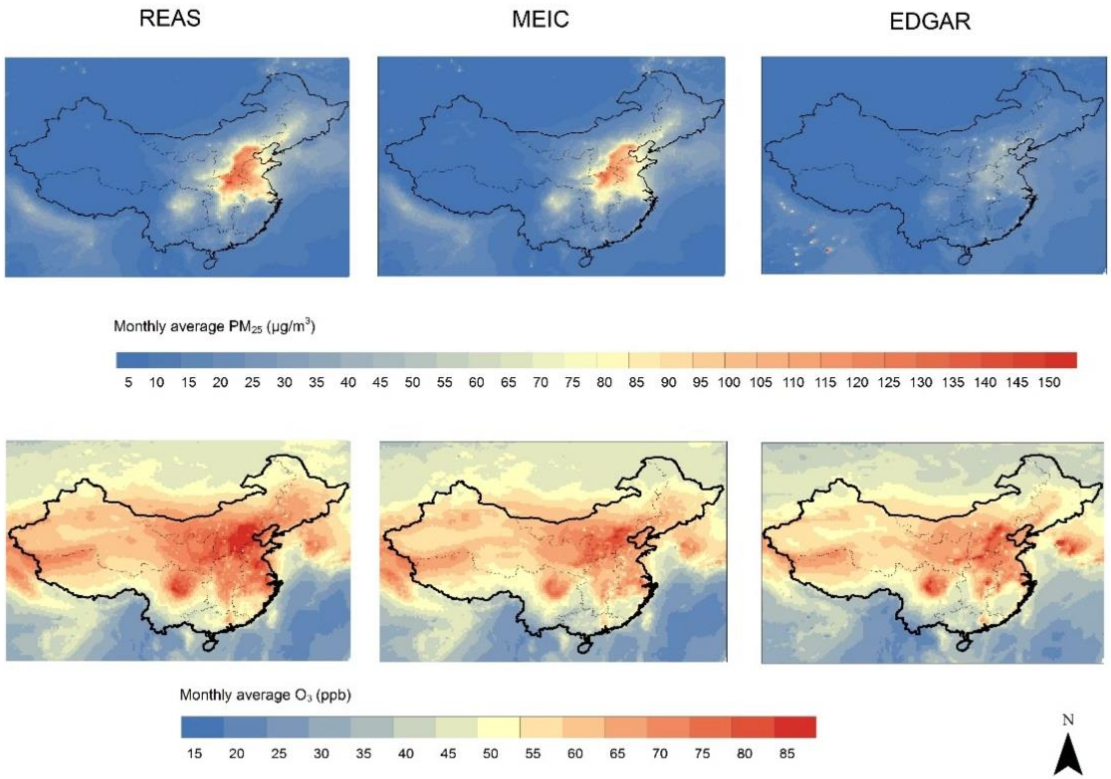

Figure 4-b. Spatial distribution of $PM_{2.5}$ and O_3 concentrations in July, 2008. Units for $PM_{2.5}$ and O_3 are $\mu g/m^3$ and ppb, respectively.

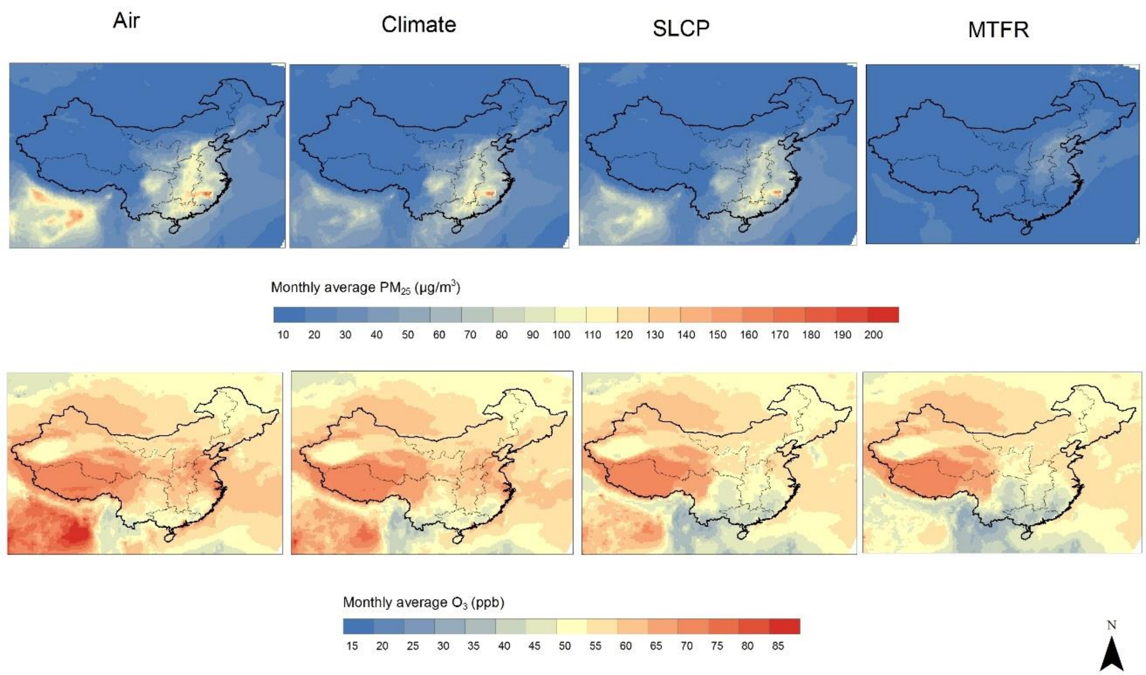

Figure 5-a. Spatial distribution of $PM_{2.5}$ and O_3 concentrations using four emission scenarios in January, 2050. Units for $PM_{2.5}$ and O_3 are μg/m^3 and ppb, respectively.

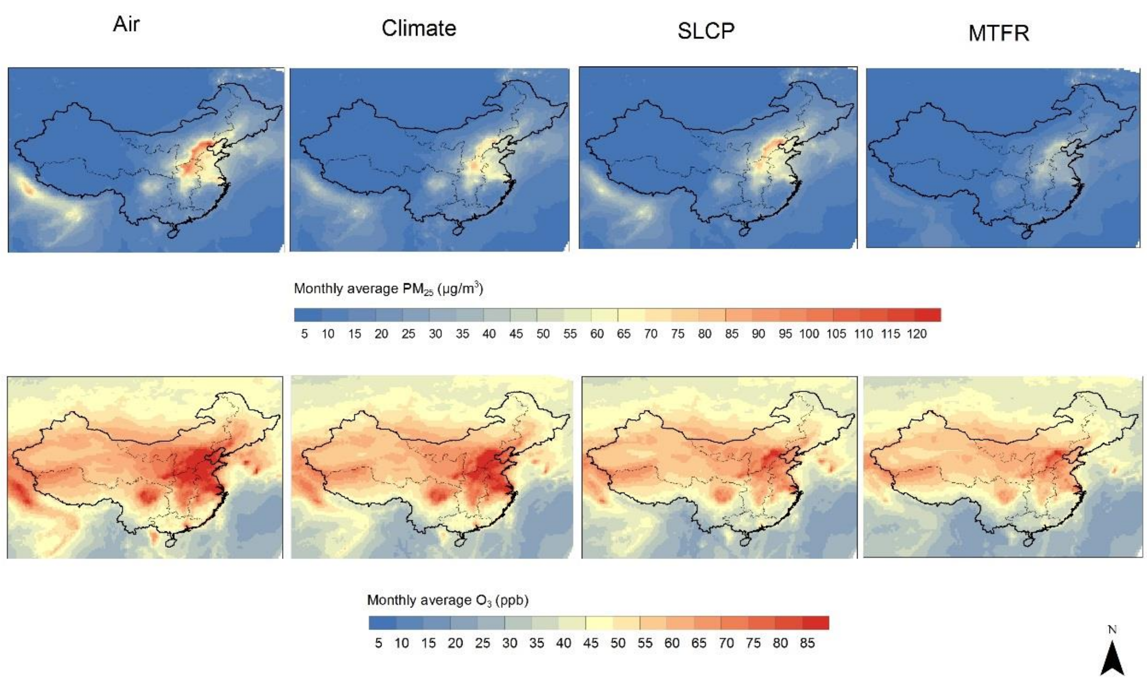

Figure 5-b. Spatial distribution of $PM_{2.5}$ and O_3 concentrations under four scenarios in July, 2050. Units for $PM_{2.5}$ and O_3 are μg/m^3 and ppb, respectively.

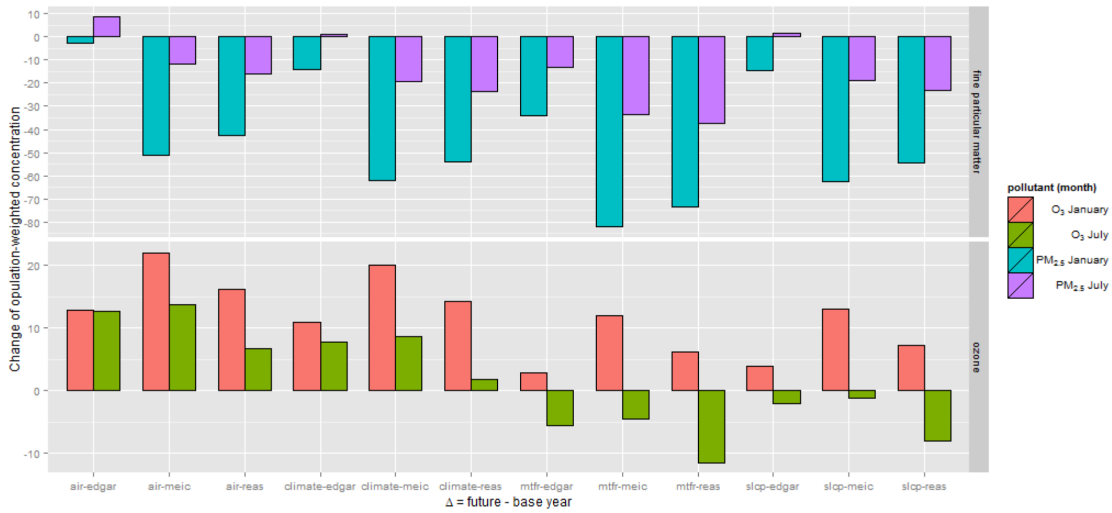

Figure 6. Change in the national population-weighted $PM_{2.5}$ and O_3 concentrations in January and July, between 2008 and 2050. Units for $PM_{2.5}$ and O_3 are μg/m^3 per person and ppb per person, respectively. The concentrations used for 2050 show M.V. population scenario. Numbers greater than zero represent an increase in pollutants, and numbers less than zero indicate a decrease in concentrations from 2008 to 2050. Upper chart shows $PM_{2.5}$, and lower chart exhibits O_3. The left bar represents January, and the right bar represents July.

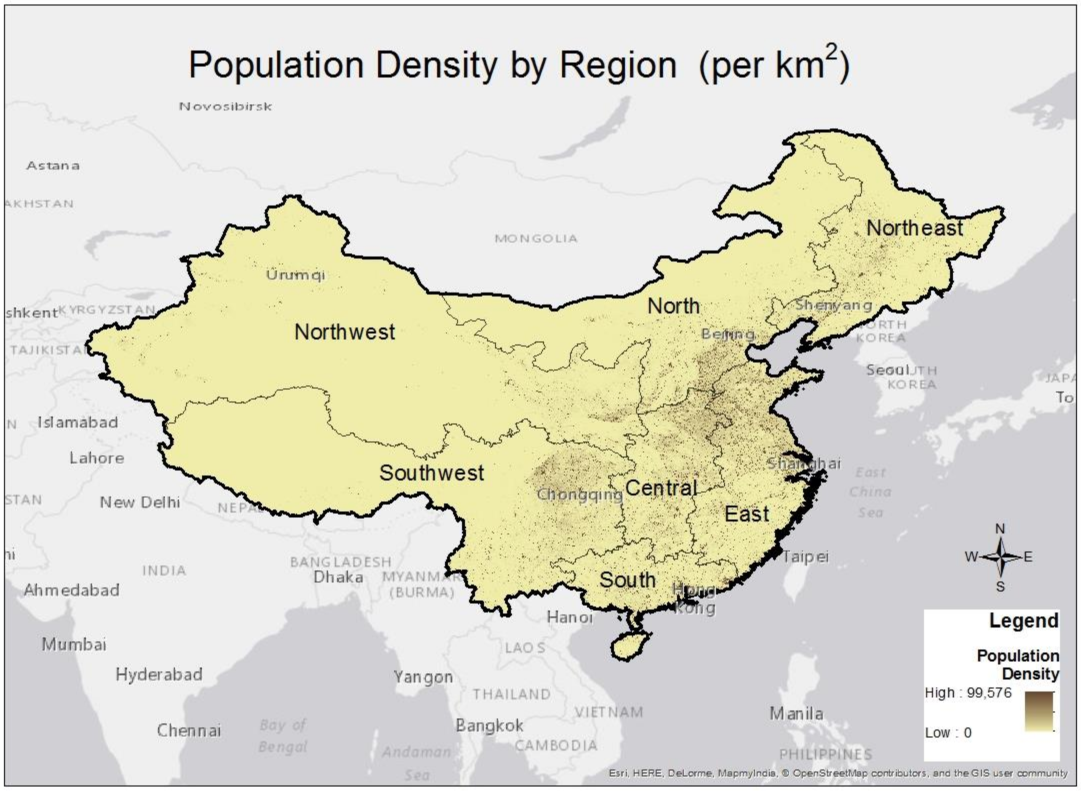

Figure 7. Population density in the Mainland China.

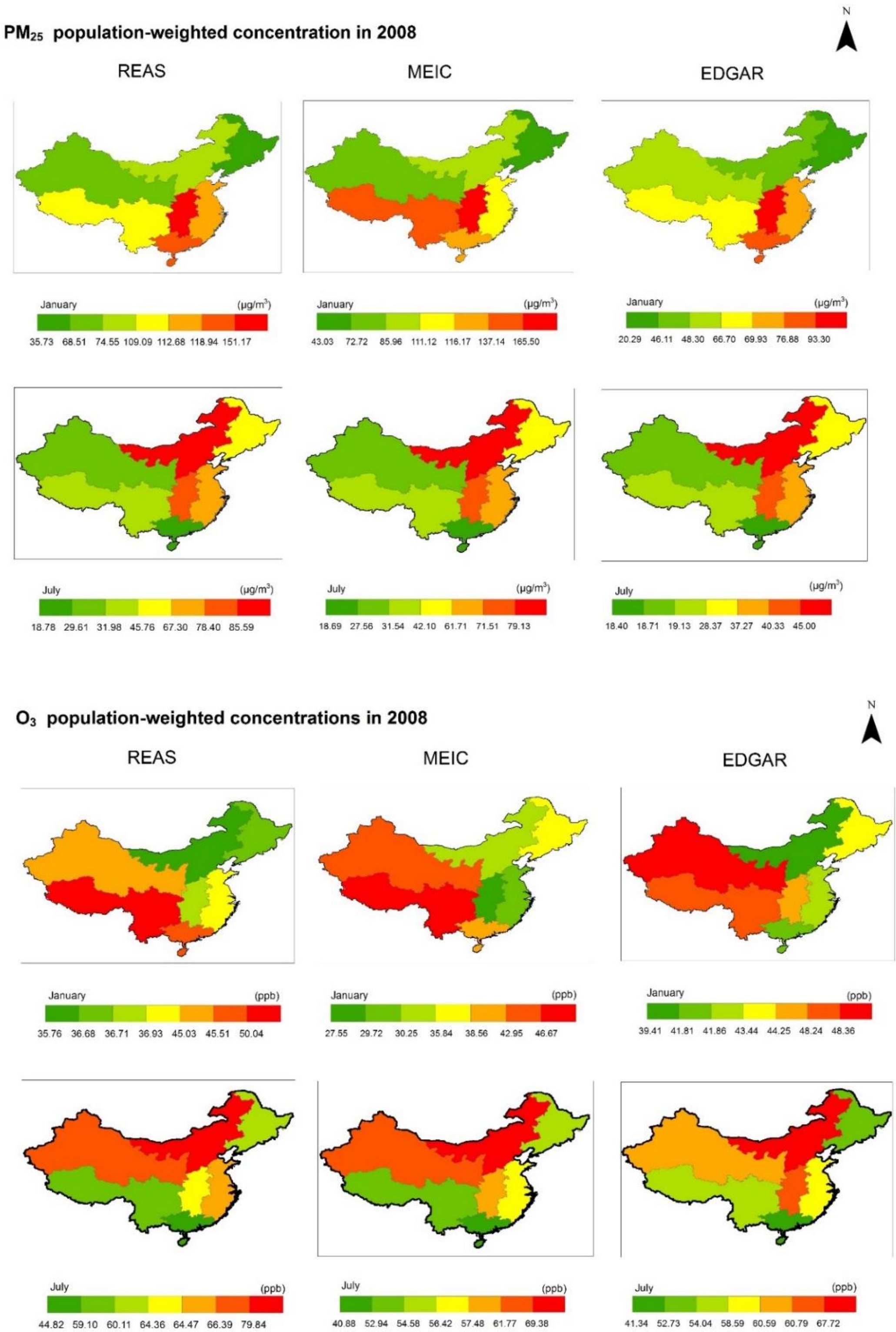

Figure 8. Regional population-weighted $PM_{2.5}$ and O_3 concentrations in January and July. Units for $PM_{2.5}$ and O_3 are μg/m^3 per person and ppb per person, respectively. Each color component in the ramp has a unique value representing the population-weighted concentrations in that specific region.

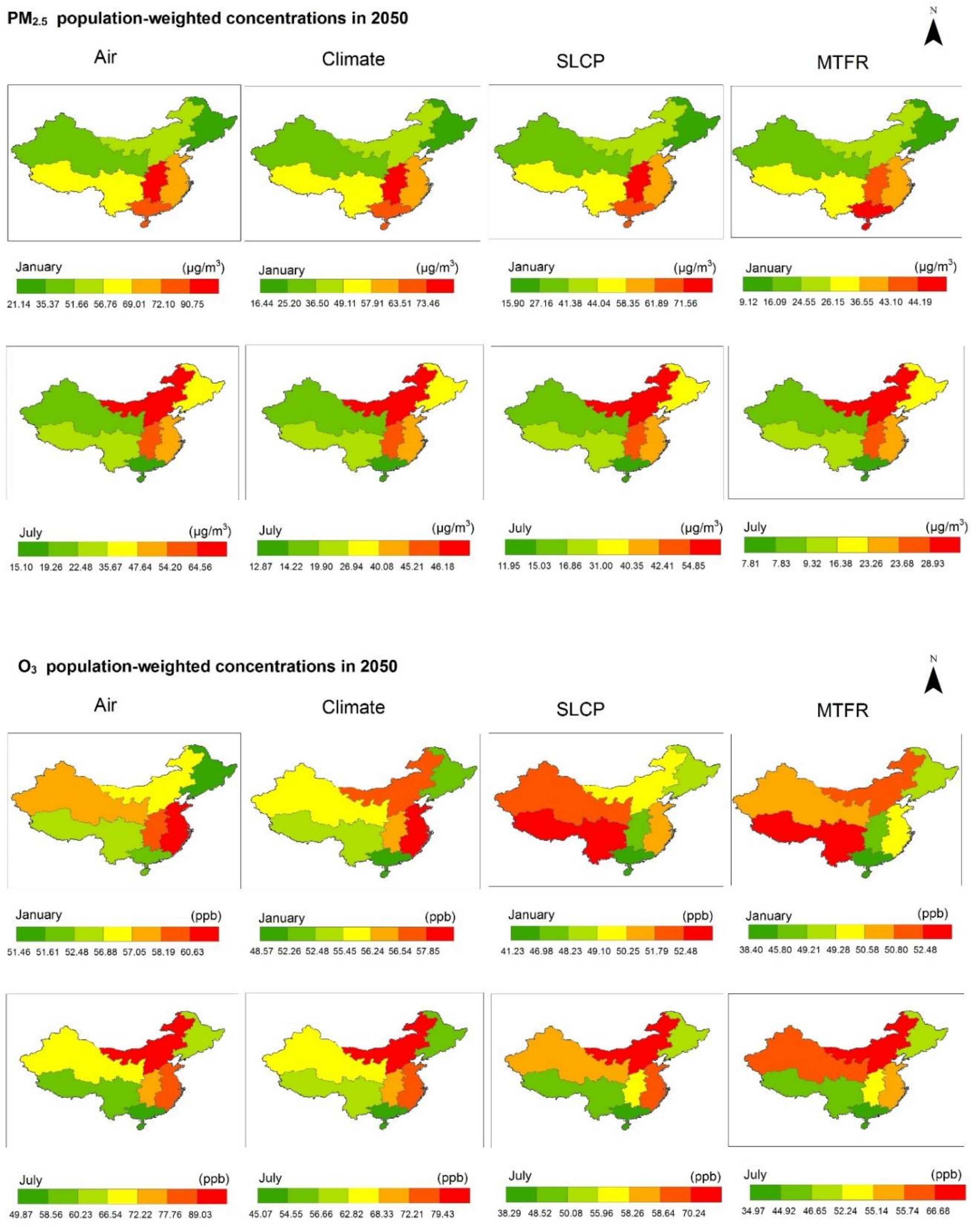

Figure 9. Regional population-weighted $PM_{2.5}$ and O_3 concentrations in January and July under M.V. scenario. Units for $PM_{2.5}$ and O_3 are μg/m^3 per person and ppb per person, respectively.

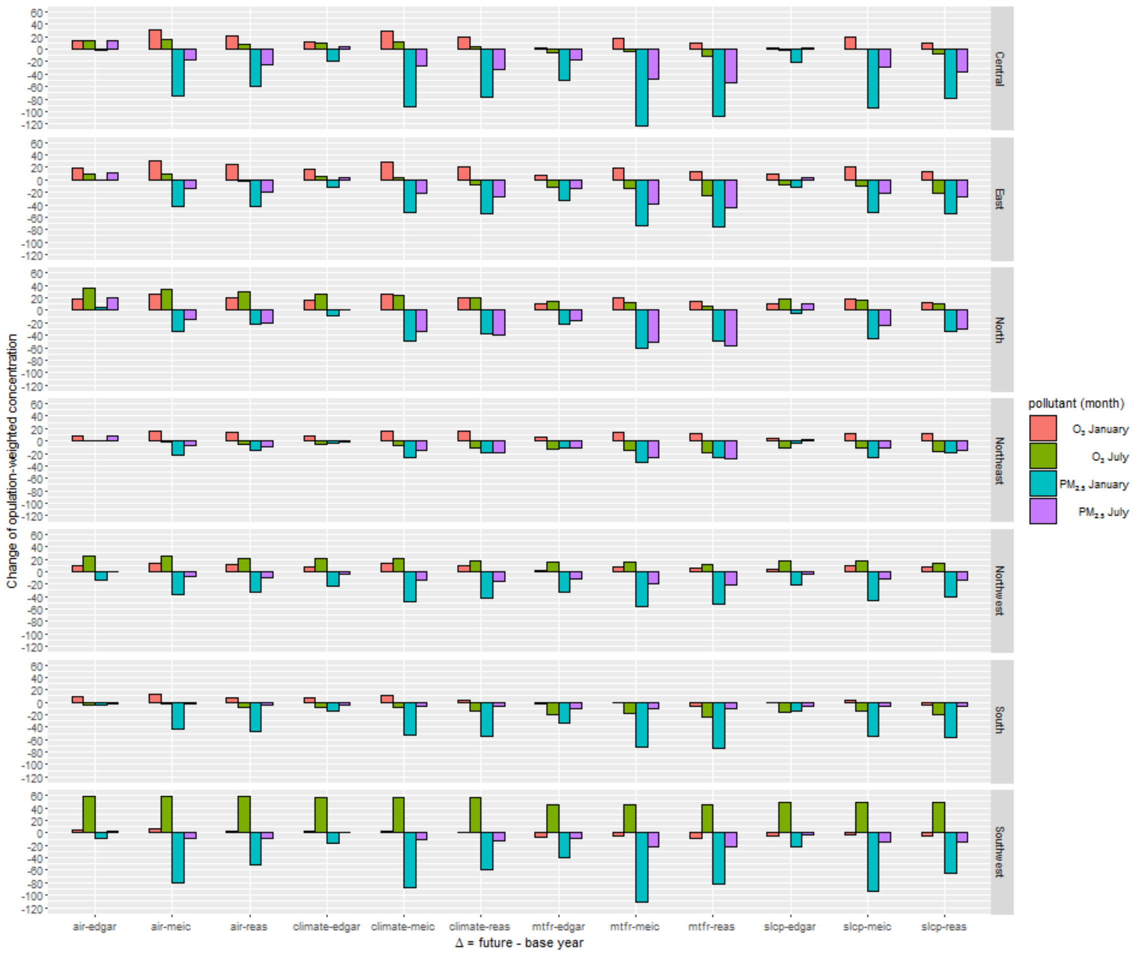

Figure 10. Regional change in the population-weighted $PM_{2.5}$ and O_3 concentrations in January and July, between 2008 and 2050. Units for $PM_{2.5}$ and O_3 are μg/m^3 per person and ppb per person, respectively. The concentrations used for 2050 are shown in M.V. population scenario. A number over zero illustrates an increase and a number less than zero represents a decrease in pollutant concentrations. O_3 concentrations in January (July) are shown in red (green), and $PM_{2.5}$ concentrations in January (July) are shown in blue (purple).

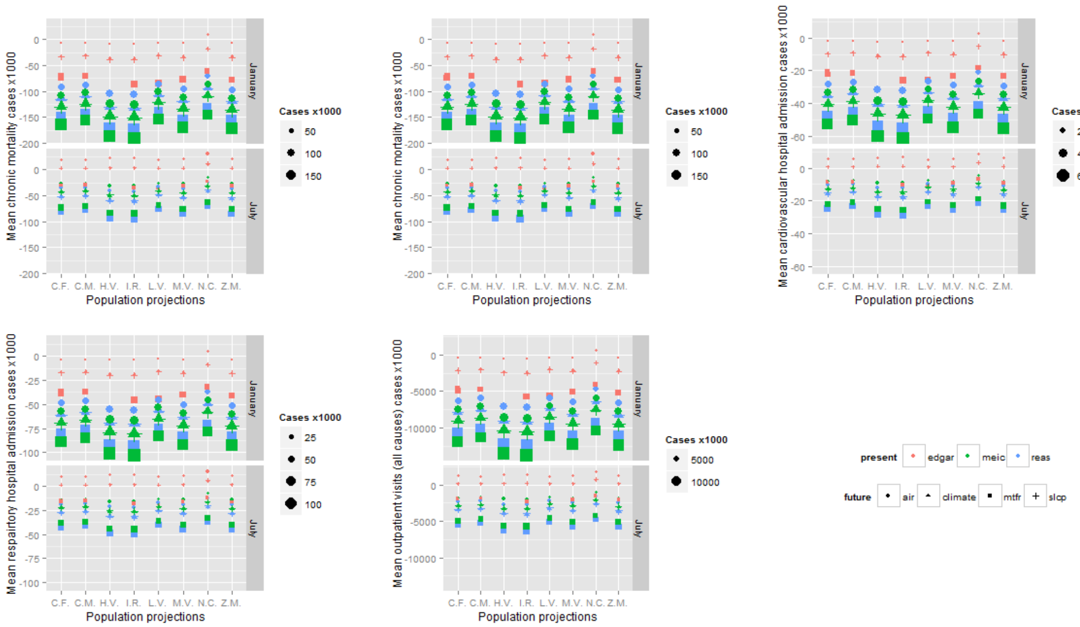

Figure 11-a. Estimated monthly mortality and morbidity cases (*1000) from $PM_{2.5}$ exposure in 2050 compared with the base year, 2008. Colors are the base year emission scenarios, and shapes are the future emissions. Red represents EDGAR, green represents MEIC, and blue represents REAS; Circle is Air, triangle is Climate, square is MTFR, and cross is SLCP. The number less than zero means cases avoided, and the number larger than zero illustrates cases attributed. The larger the symbols are, the more absolute value of cases avoided/attributed.

Abbreviation: C.F.: Constant fertility; C.M.: Constant mortality; H.V.: High variant; I.R.: Instant replacement; L.V.: Low variant; M.V.: Medium variant; N.C.: No change; Z.M.: Zero Migration

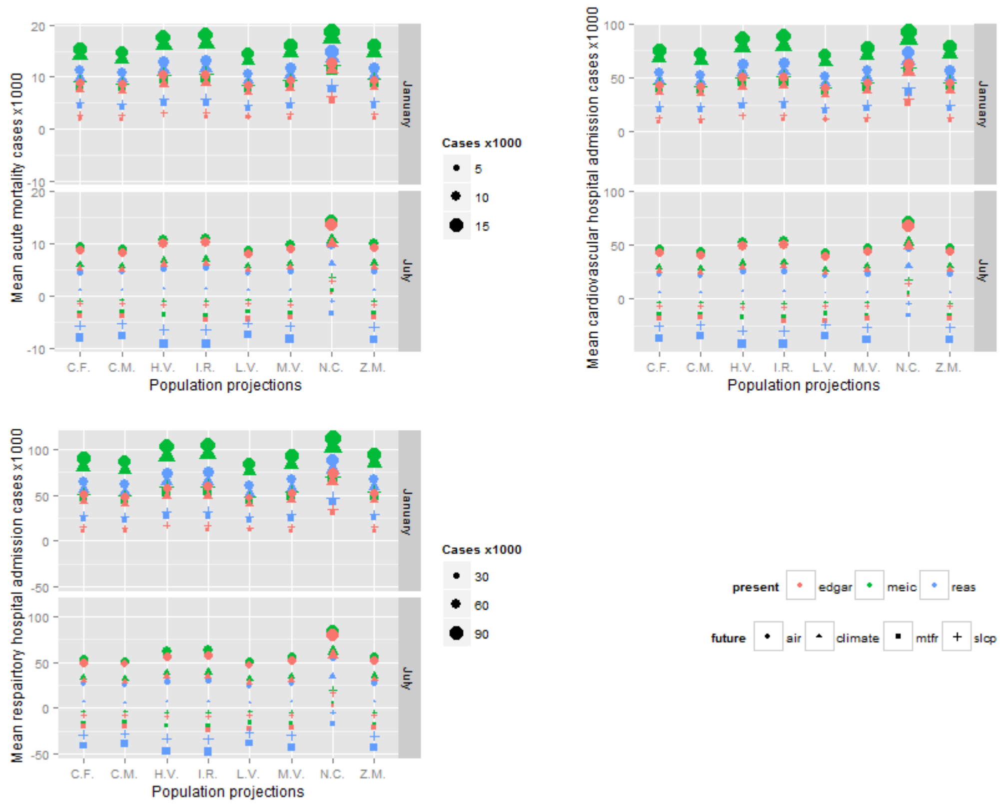

Figure 11-b. Estimated monthly mortality and morbidity cases (*1000) from O_3 exposure in 2050 compared with the base year, 2008. Colors are the base year emission scenarios, and shapes are the future emissions. Red represents EDGAR, green represents MEIC, and blue represents REAS; Circle is Air, triangle is Climate, square is MTFR, and cross is SLCP. The number less than zero means cases avoided, and the number larger than zero illustrates cases attributed. The larger the symbols are, the more absolute value of cases avoided/attributed.

Abbreviation: C.F.: Constant fertility; C.M.: Constant mortality; H.V.: High variant; I.R.: Instant replacement; L.V.: Low variant; M.V: Medium variant; N.C.: No change; Z.M: Zero Migration

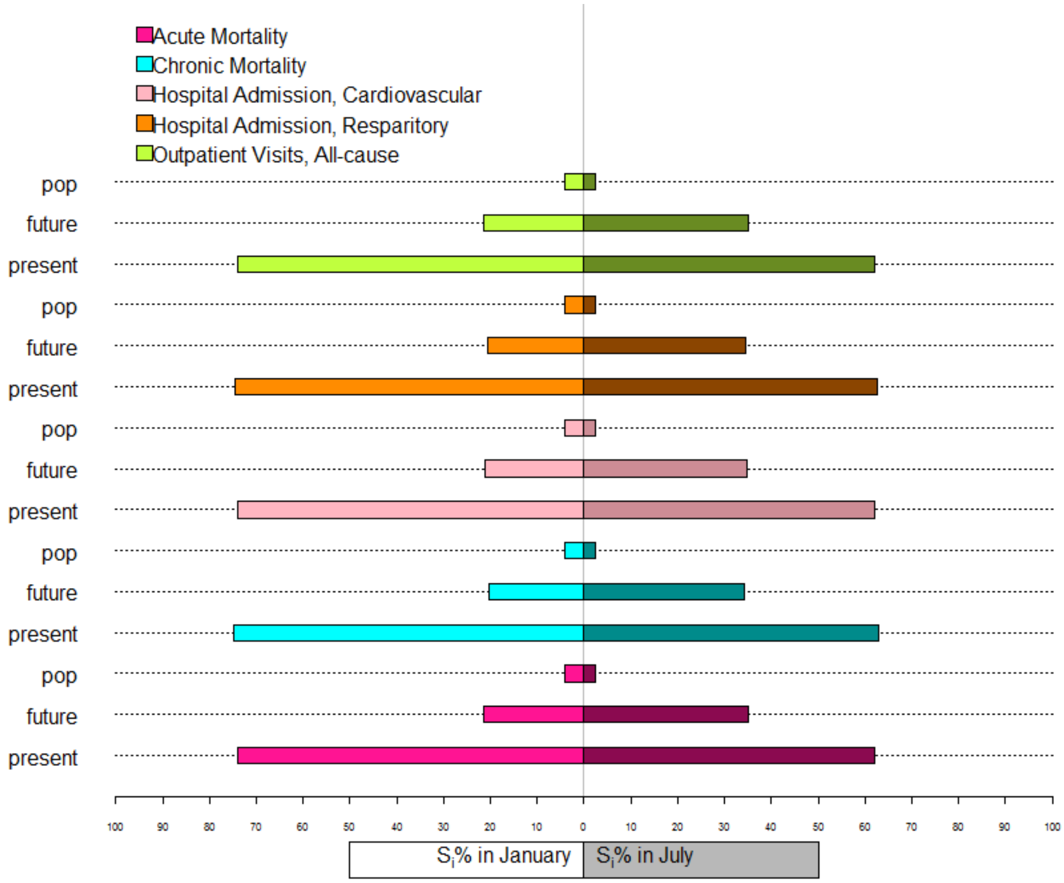

Figure 12-a. Sensitivity analysis of $PM_{2.5}$-related national mean mortality and morbidity in the Mainland China resulted by base year emission inventory inputs (present), future emission scenario uses (future), and population projections (pop). Percentage of the sensitivity index (Si%) is the indicator of the attributed uncertainty to the total variance. Higher Si% value indicates a larger source of uncertainty. Lighter color represents January and darker color represents July.

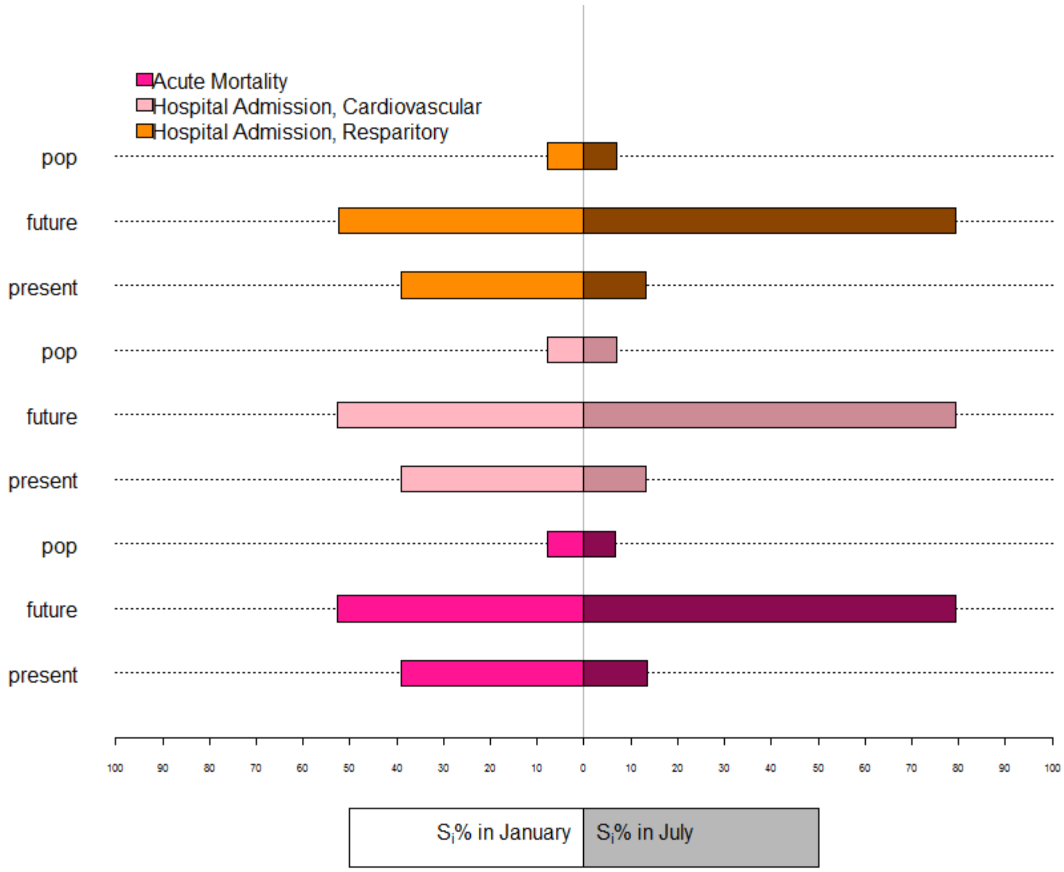

Figure 11-b. Sensitivity analysis of O_3 related national mean mortality and morbidity in the Mainland China resulted by base year emission inventory inputs (present), future emission scenario uses (future), and population projections (pop). Percentage of the sensitivity index (Si%) is the indicator of the attributed uncertainty to the total variance. Higher Si% value indicates a larger source of uncertainty. Lighter color represents January and darker color represents July.

Appendix

Table A-1(a). Risk ratio (RR) and 95% Confidence Interval (CI) for mortality and morbidity if $PM_{2.5}$ concentrations increased by 10 μg/m^3

Health Endpoints	RR (95% CI)	Reference
Acute mortality	1.0065 (1.0050-1.0070)	Lei (2013)
Chronic mortality	1.04 (1.01-1.08)	Pope et al. (2002)
Hospital admissions, cardiovascular	1.01 (1.0033, 1.0184)	T.W.Wong et al. (1999)
Hospital admissions, respiratory	1.0268 (1.0167,1.0369)	T.W.Wong et al. (1999)
Outpatient visits, all causes	1.0039 (1.0024,1.0052)	Xu, Li and Huang (1995)

Note: Risk ratios for $PM_{2.5}$ are based on the assumption that the ratio of $PM_{2.5}$ to PM_{10} is 0.6 and the ratio of PM_{10} to total suspended particulate (TSP) is 0.5

Table A-1(b). Risk ratio (RR) and 95% Confidence Interval (CI) for mortality and morbidity if O_3 concentrations increased by 10 μg/m^3

Health Endpoints	RR (95% CI)	Reference
Acute mortality	1.0031(1.0013,1.0048)	Wong et al. (2008)
Hospital admissions, cardiovascular	1.0496 (1.0189, 1.0811)	T.W.Wong et al. (1999)
Hospital admissions, respiratory	1.0850 (1.0574,1.1132)	T.W.Wong et al. (1999)

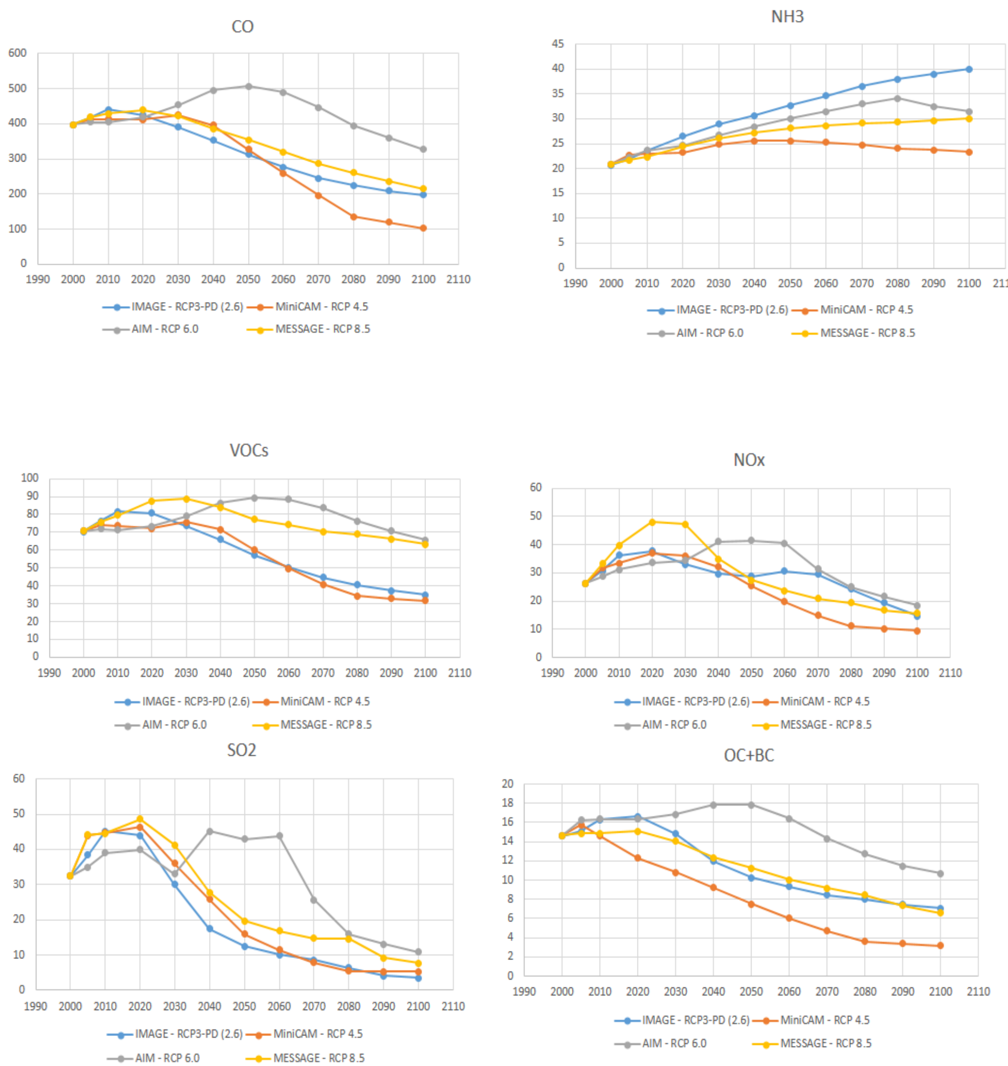

Figure A-1. IPCC emission comparisons

Table A-2. National population weighted $PM_{2.5}$ and O_3 concentrations in 2008; Unit for $PM_{2.5}$ is μg/m^3 per person. Unit for O_3 is ppb per person. Numbers are rounded to the nearest hundredth

Air pollutants (Month)	REAS	MEIC	EDGAR
$PM_{2.5}$ (January)	105.30	113.64	65.68
$PM_{2.5}$ (July)	56.04	51.94	31.74
O_3 (January)	40.29	34.47	43.57
O_3 (July)	63.04	56.11	57.09

Table A-3(a). National population weighted $PM_{2.5}$ concentrations in January 2050, under eight population projections; Unit for $PM_{2.5}$ is μg/m^3 per person. Numbers are rounded to the nearest ten-thousandth

Population projection	Air	Climate	SLCP	MTFR
Medium Variant	62.7060	51.4755	50.9804	31.7097
High Variant	62.7060	51.4755	50.9804	31.7097
Low Variant	62.7060	51.4755	50.9804	31.7097
Contant Fertility	62.7060	51.4755	50.9804	31.7097
Instant Replacement	62.7060	51.4755	50.9804	31.7097
Zero Migration	62.7060	51.4755	50.9804	31.7097
Constant Mortality	62.7060	51.4755	50.9804	31.7097
No Change	70.4160	57.8046	57.2486	35.6086

Table A-3(b). National population weighted $PM_{2.5}$ concentrations in July, 2050 under eight population projections; Unit for $PM_{2.5}$ is μg/m^3 per person. Numbers are rounded to the nearest ten-thousandth

Population projection	Air	Climate	SLCP	MTFR
Medium Variant	40.2435	32.5975	33.0418	18.4487
High Variant	40.2435	32.5975	33.0418	18.4487
Low Variant	40.2435	32.5975	33.0418	18.4487
Constant Fertility	40.2435	32.5975	33.0418	18.4487
Instant Replacement	40.2435	32.5975	33.0418	18.4487
Zero Migration	40.2435	32.5975	33.0418	18.4487
Constant Mortality	40.2435	32.5975	33.0418	18.4487
No Change	45.1916	36.6055	37.1045	20.7171

Table A-3(c). National population weighted O_3 concentrations in January, 2050 under eight population projections; Unit for O_3 is ppb per person. Numbers are rounded to the nearest ten-thousandth

Population projection	Air	Climate	SLCP	MTFR
Medium Variant	56.4802	54.5263	47.5289	46.4780
High Variant	56.4802	54.5263	47.5289	46.4780
Low Variant	56.4802	54.5263	47.5289	46.4780
Constant Fertility	56.4802	54.5263	47.5289	46.4780
Instant Replacement	56.4802	54.5263	47.5289	46.4780
Zero Migration	56.4802	54.5263	47.5289	46.4780
Constant Mortality	56.4802	54.5263	47.5289	46.4780
No Change	63.4247	61.2305	53.3728	52.1927

Table A-3(d). National population weighted O_3 concentrations in July, 2050 under eight population projections; Unit for O_3 is ppb per person. Numbers are rounded to the nearest ten-thousandth

Population projection	Air	Climate	SLCP	MTFR
Medium Variant	69.7987	64.8284	54.9844	51.5226
High Variant	69.7987	64.8284	54.9844	51.5226
Low Variant	69.7987	64.8284	54.9844	51.5227
Constant Fertility	69.7987	64.8284	54.9844	51.5227
Instant Replacement	69.7987	64.8284	54.9844	51.5227
Zero Migration	69.7987	64.8284	54.9844	51.5226
Constant Mortality	69.7987	64.8284	54.9844	51.5227
No Change	78.3807	72.7994	61.7450	57.8576

Table A-4. Regional population weighted $PM_{2.5}$ and O_3 concentrations in January and July, 2008; Unit for $PM_{2.5}$ is μg/m^3 per person Unit for O_3 is ppb per person. Numbers are rounded to the nearest ten-thousandth

							$PM_{2.5}$ January
	Central	East	North	Northeast	Northwest	South	Southwest
REAS	151.17	112.68	74.55	35.73	68.51	118.94	109.09
MEIC	165.50	111.12	85.96	43.03	72.72	116.17	137.14
EDGAR	93.30	69.93	46.11	20.29	48.30	76.88	66.70
							$PM_{2.5}$ July
REAS	78.40	67.30	85.59	45.76	29.61	18.78	31.98
MEIC	71.51	61.71	79.13	42.10	27.56	18.69	31.54
EDGAR	40.33	37.27	45.00	28.37	18.71	18.40	19.13
							O_3 January
REAS	36.71	36.93	35.76	36.68	45.03	45.51	50.04
MEIC	27.55	29.72	30.25	35.84	42.95	38.56	46.67
EDGAR	44.25	41.86	39.41	43.44	48.36	41.81	48.24
							O_3 July
REAS	64.36	64.47	79.84	60.11	66.39	44.82	59.10
MEIC	57.48	56.42	69.38	54.58	61.77	40.88	52.94
EDGAR	60.79	58.59	67.72	52.73	60.59	41.34	54.04

Table A-5(a). Projected regional population weighted $PM_{2.5}$ concentrations in January 2050; Unit for $PM_{2.5}$ is μg/m^3 per person. Numbers are rounded to the nearest ten-thousandth

Emission scenario	Population projection	Central	East	North	Northeast	Northwest	South	Southwest
Air	Medium Variant	90.7510	69.0112	51.6627	21.1431	35.3697	72.0990	56.7589
	High Variant	90.7510	69.0112	51.6627	21.1431	35.3697	72.0990	56.7589
	Low Variant	90.7510	69.0112	51.6627	21.1431	35.3696	72.0990	56.7589
	Constant Fertility	90.7510	69.0112	51.6627	21.1431	35.3696	72.0990	56.7589
	Instant Replacement	90.7510	69.0112	51.6627	21.1431	35.3697	72.0990	56.7589
	Zero Migration	90.7510	69.0112	51.6627	21.1431	35.3697	72.0990	56.7589
	Constant Mortality	90.7510	69.0112	51.6627	21.1431	35.3696	72.0990	56.7589
	No Change	90.7510	69.0112	51.6627	21.1431	35.3696	72.0990	56.7589
Climate	Medium Variant	73.4643	57.9078	36.4989	16.4356	25.2035	63.5141	49.1113
	High Variant	73.4643	57.9078	36.4988	16.4356	25.2034	63.5141	49.1113
	Low Variant	73.4644	57.9078	36.4988	16.4356	25.2034	63.5141	49.1113
	Constant Fertility	73.4644	57.9078	36.4988	16.4356	25.2034	63.5141	49.1112
	Instant Replacement	73.4643	57.9078	36.4988	16.4356	25.2034	63.5141	49.1113
	Zero Migration	73.4644	57.9078	36.4989	16.4356	25.2034	63.5141	49.1113
	Constant Mortality	73.4644	57.9078	36.4988	16.4356	25.2034	63.5141	49.1112
	No Change	73.4644	57.9078	36.4988	16.4356	25.2034	63.5141	49.1112
SLCP	Medium Variant	71.5647	58.3534	41.3795	15.9005	27.1604	61.8862	44.0442
	High Variant	71.5647	58.3534	41.3795	15.9005	27.1604	61.8862	44.0442
	Low Variant	71.5647	58.3534	41.3795	15.9005	27.1603	61.8862	44.0442
	Constant Fertility	71.5647	58.3534	41.3795	15.9005	27.1603	61.8862	44.0441

	Instant Replacement	71.5647	58.3534	41.3795	15.9005	27.1603	61.8862	44.0442
	Zero Migration	71.5647	58.3534	41.3795	15.9005	27.1604	61.8862	44.0442
	Constant Mortality	71.5647	58.3534	41.3795	15.9005	27.1603	61.8862	44.0441
	No Change	71.5647	58.3534	41.3795	15.9005	27.1603	61.8862	44.0441
MTFR	Medium Variant	43.1031	36.5548	24.5471	9.1157	16.0853	44.1885	26.1537
	High Variant	43.1031	36.5548	24.5471	9.1157	16.0852	44.1885	26.1537
	Low Variant	43.1031	36.5548	24.5471	9.1157	16.0852	44.1885	26.1537
	Constant Fertility	43.1031	36.5548	24.5471	9.1157	16.0852	44.1885	26.1537
	Instant Replacement	43.1031	36.5548	24.5471	9.1157	16.0852	44.1885	26.1537
	Zero Migration	43.1031	36.5548	24.5471	9.1157	16.0852	44.1885	26.1537
	Constant Mortality	43.1031	36.5548	24.5471	9.1157	16.0852	44.1885	26.1537
	No Change	43.1031	36.5548	24.5471	9.1157	16.0852	44.1885	26.1537

Table A-5(b). Projected regional population weighted $PM_{2.5}$ concentrations in July 2050; Unit for $PM_{2.5}$ is $\mu g/m^3$ per person. Numbers are rounded to the nearest ten-thousandth

Emission scenario	Population projection	Central	East	North	Northeast	Northwest	South	Southwest
Air	Medium Variant	54.2036	47.6440	64.5607	35.6729	19.2591	15.1047	22.4811
	High Variant	54.2036	47.6440	64.5606	35.6729	19.2590	15.1047	22.4811
	Low Variant	54.2036	47.6440	64.5606	35.6729	19.2590	15.1047	22.4811
	Constant Fertility	54.2036	47.6440	64.5606	35.6729	19.2590	15.1047	22.4811
	Instant Replacement	54.2036	47.6440	64.5606	35.6729	19.2590	15.1047	22.4811
	Zero Migration	54.2036	47.6440	64.5606	35.6729	19.2590	15.1047	22.4811
	Constant Mortality	54.2036	47.6440	64.5606	35.6729	19.2590	15.1047	22.4811
	No Change	54.2036	47.6440	64.5606	35.6729	19.2590	15.1047	22.4811
Climate	Medium Variant	45.2057	40.0809	46.1778	26.9379	14.2172	12.8692	19.8977
	High Variant	45.2057	40.0809	46.1778	26.9379	14.2171	12.8692	19.8977
	Low Variant	45.2057	40.0809	46.1778	26.9379	14.2171	12.8692	19.8977
	Constant Fertility	45.2057	40.0809	46.1778	26.9379	14.2171	12.8692	19.8977
	Instant Replacement	45.2057	40.0809	46.1778	26.9379	14.2171	12.8692	19.8977
	Zero Migration	45.2057	40.0809	46.1778	26.9379	14.2171	12.8692	19.8977
	Constant Mortality	45.2057	40.0809	46.1778	26.9379	14.2171	12.8692	19.8977
	No Change	45.2057	40.0809	46.1778	26.9379	14.2171	12.8692	19.8977
SLCP	Medium Variant	42.4054	40.3489	54.8550	31.0042	15.0289	11.9529	16.8564
	High Variant	42.4054	40.3489	54.8549	31.0042	15.0288	11.9529	16.8564
	Low Variant	42.4054	40.3489	54.8549	31.0042	15.0288	11.9529	16.8564
	Constant Fertility	42.4054	40.3489	54.8549	31.0042	15.0288	11.9529	16.8564

	Instant Replacement	42.4054	40.3489	54.8549	31.0042	15.0288	11.9529	16.8564
	Zero Migration	42.4054	40.3489	54.8550	31.0042	15.0289	11.9529	16.8564
	Constant Mortality	42.4054	40.3489	54.8549	31.0042	15.0288	11.9529	16.8564
	No Change	42.4054	40.3489	54.8549	31.0042	15.0288	11.9529	16.8564
MTFR	Medium Variant	23.6763	23.2553	28.9286	16.3817	7.8275	7.8078	9.3179
	High Variant	23.6763	23.2553	28.9286	16.3817	7.8275	7.8078	9.3179
	Low Variant	23.6763	23.2553	28.9286	16.3817	7.8275	7.8078	9.3179
	Constant Fertility	23.6763	23.2553	28.9286	16.3817	7.8275	7.8078	9.3179
	Instant Replacement	23.6763	23.2553	28.9286	16.3817	7.8275	7.8078	9.3179
	Zero Migration	23.6763	23.2553	28.9286	16.3817	7.8275	7.8078	9.3179
	Constant Mortality	23.6763	23.2553	28.9286	16.3817	7.8275	7.8078	9.3179
	No Change	23.6763	23.2553	28.9286	16.3817	7.8275	7.8078	9.3179

Table A-5(c). Projected regional population weighted O_3 concentrations in January, 2050 under eight population projections; Unit for O_3 is ppb per person. Numbers are rounded to the nearest ten-thousandth

Emission scenario	Population projection	Central	East	North	Northeast	Northwest	South	Southwest
Air	Medium Variant	58.1922	60.6286	56.8805	51.4619	57.0547	51.6112	52.4846
	High Variant	58.1922	60.6286	56.8805	51.4619	57.0547	51.6112	52.4846
	Low Variant	58.1922	60.6286	56.8805	51.4619	57.0547	51.6112	52.4846
	Constant Fertility	58.1922	60.6286	56.8805	51.4619	57.0547	51.6112	52.4846
	Instant Replacement	58.1922	60.6286	56.8805	51.4619	57.0547	51.6112	52.4846
	Zero Migration	58.1922	60.6286	56.8805	51.4619	57.0547	51.6112	52.4846
	Constant Mortality	58.1922	60.6286	56.8805	51.4619	57.0547	51.6112	52.4846
	No Change	58.1922	60.6286	56.8805	51.4619	57.0547	51.6112	52.4846
Climate	Medium Variant	56.2426	57.8477	56.5405	52.2647	55.4467	48.5742	49.9403
	High Variant	56.2426	57.8477	56.5405	52.2647	55.4467	48.5742	49.9403
	Low Variant	56.2426	57.8477	56.5405	52.2647	55.4467	48.5742	49.9403
	Constant Fertility	56.2426	57.8477	56.5405	52.2647	55.4467	48.5742	49.9403
	Instant Replacement	56.2426	57.8477	56.5405	52.2647	55.4467	48.5742	49.9403
	Zero Migration	56.2426	57.8477	56.5405	52.2647	55.4467	48.5742	49.9403
	Constant Mortality	56.2426	57.8477	56.5405	52.2647	55.4467	48.5742	49.9403
	No Change	56.2426	57.8477	56.5405	52.2647	55.4467	48.5742	49.9403
SLCP	Medium Variant	46.9780	50.2538	49.1046	48.2290	51.7932	41.2312	43.9951
	High Variant	46.9780	50.2538	49.1046	48.2290	51.7933	41.2312	43.9951
	Low Variant	46.9780	50.2538	49.1046	48.2290	51.7933	41.2312	43.9951

	Constant Fertility	46.9780	50.2538	49.1046	48.2290	51.7933	41.2312	43.9951
	Instant Replacement	46.9780	50.2538	49.1046	48.2290	51.7933	41.2312	43.9951
	Zero Migration	46.9780	50.2538	49.1046	48.2290	51.7933	41.2312	43.9951
	Constant Mortality	46.9780	50.2538	49.1046	48.2290	51.7933	41.2312	43.9951
	No Change	46.9780	50.2538	49.1046	48.2290	51.7933	41.2312	43.9951
MTFR	Medium Variant	45.8011	49.2809	50.7980	49.2088	50.5772	38.3950	41.0906
	High Variant	45.8011	49.2809	50.7980	49.2088	50.5772	38.3950	41.0906
	Low Variant	45.8011	49.2809	50.7980	49.2088	50.5772	38.3950	41.0906
	Constant Fertility	45.8011	49.2809	50.7980	49.2088	50.5772	38.3950	41.0907
	Instant Replacement	45.8011	49.2809	50.7980	49.2088	50.5772	38.3950	41.0906
	Zero Migration	45.8011	49.2809	50.7980	49.2088	50.5772	38.3950	41.0906
	Constant Mortality	45.8011	49.2809	50.7980	49.2088	50.5772	38.3950	41.0906
	No Change	45.8011	49.2809	50.7980	49.2088	50.5772	38.3950	41.0906

Table A-5(d). Projected regional population weighted O_3 concentrations in July, 2050 under eight population projections; Unit for O_3 is ppb per person. Numbers are rounded to the nearest ten-thousandth

Emission scenario	Population projection	Central	East	North	Northeast	Northwest	South	Southwest
Air	Medium Variant	72.2169	77.7624	89.0283	60.2299	66.5369	49.8675	58.5576
	High Variant	72.2169	77.7624	89.0283	60.2299	66.5369	49.8675	58.5576
	Low Variant	72.2169	77.7624	89.0283	60.2299	66.5369	49.8675	58.5576
	Constant Fertility	72.2169	77.7624	89.0283	60.2299	66.5369	49.8675	58.5576
	Instant Replacement	72.2169	77.7624	89.0283	60.2299	66.5369	49.8675	58.5576
	Zero Migration	72.2169	77.7624	89.0283	60.2299	66.5369	49.8675	58.5576
	Constant Mortality	72.2169	77.7624	89.0283	60.2299	66.5369	49.8675	58.5576
	No Change	72.2169	77.7624	89.0283	60.2299	66.5369	49.8675	58.5576
Climate	Medium Variant	68.3315	72.2123	79.4285	54.5519	62.8175	45.0666	56.6561
	High Variant	68.3315	72.2123	79.4284	54.5519	62.8174	45.0666	56.6561
	Low Variant	68.3315	72.2123	79.4284	54.5519	62.8174	45.0666	56.6561
	Constant Fertility	68.3315	72.2123	79.4284	54.5519	62.8174	45.0666	56.6561
	Instant Replacement	68.3315	72.2123	79.4284	54.5519	62.8174	45.0666	56.6561
	Zero Migration	68.3315	72.2123	79.4285	54.5519	62.8175	45.0666	56.6560
	Constant Mortality	68.3315	72.2123	79.4285	54.5519	62.8174	45.0666	56.6560
	No Change	68.3315	72.2123	79.4284	54.5519	62.8174	45.0666	56.6560
SLCP	Medium Variant	55.9562	58.6354	70.2415	50.0807	58.2647	38.2906	48.5159
	High Variant	55.9562	58.6354	70.2415	50.0807	58.2647	38.2906	48.5159
	Low Variant	55.9562	58.6354	70.2415	50.0807	58.2646	38.2906	48.5159
	Constant Fertility	55.9562	58.6354	70.2415	50.0807	58.2646	38.2906	48.5159

	Instant Replacement	55.9562	58.6354	70.2415	50.0807	58.2647	38.2906	48.5159
	Zero Migration	55.9562	58.6354	70.2415	50.0807	58.2647	38.2906	48.5159
	Constant Mortality	55.9562	58.6354	70.2415	50.0807	58.2646	38.2906	48.5159
	No Change	55.9562	58.6354	70.2415	50.0807	58.2646	38.2906	48.5159
MTFR	Medium Variant	52.2421	55.1444	66.6763	46.6491	55.7443	34.9681	44.9178
	High Variant	52.2421	55.1444	66.6762	46.6491	55.7443	34.9681	44.9178
	Low Variant	52.2421	55.1444	66.6762	46.6491	55.7443	34.9681	44.9178
	Constant Fertility	52.2421	55.1444	66.6762	46.6491	55.7443	34.9681	44.9178
	Instant Replacement	52.2421	55.1444	66.6762	46.6491	55.7443	34.9681	44.9178
	Zero Migration	52.2421	55.1444	66.6762	46.6491	55.7443	34.9681	44.9178
	Constant Mortality	52.2421	55.1444	66.6762	46.6491	55.7443	34.9681	44.9178
	No Change	52.2421	55.1444	66.6762	46.6491	55.7443	34.9681	44.9178

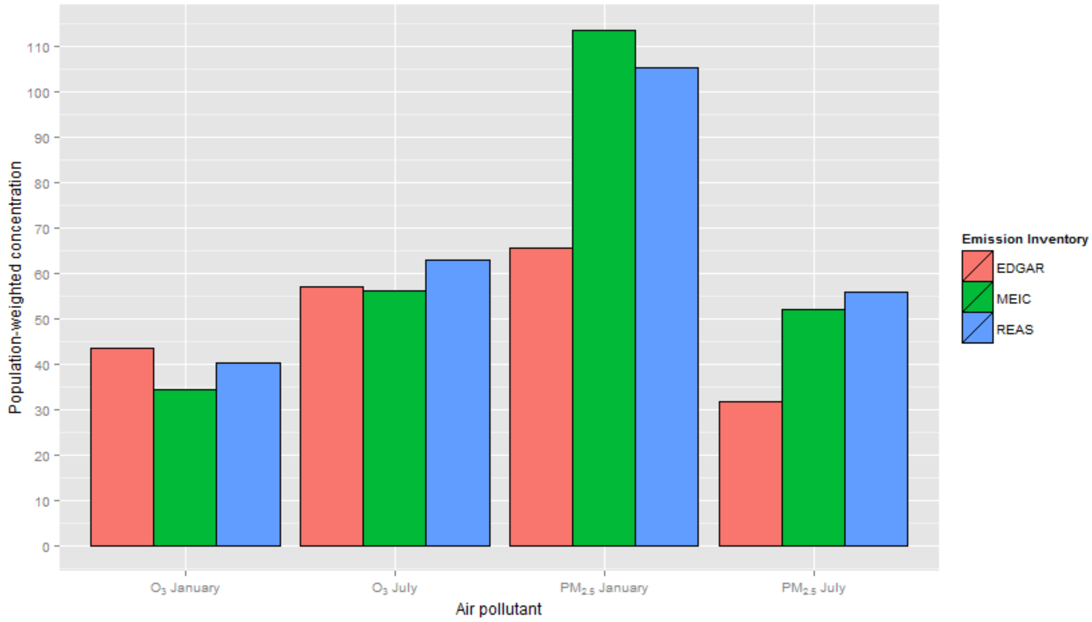

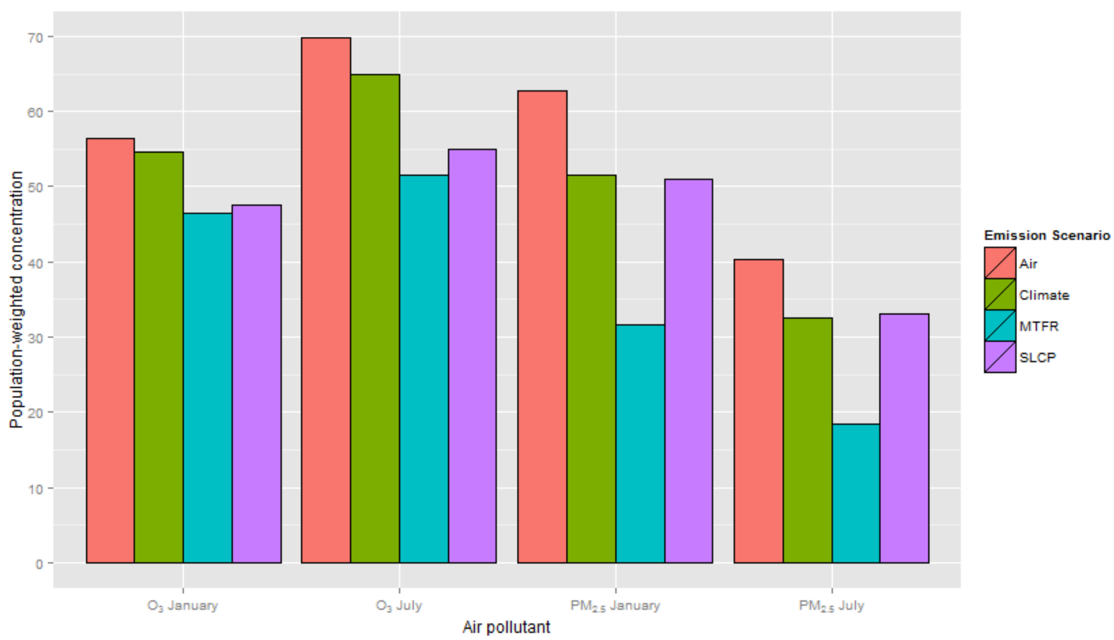

Figure A-2. National population-weighted $PM_{2.5}$ and O_3 concentrations in January and July. Units for $PM_{2.5}$ and O_3 are $\mu g/m^3$ per person and ppb per person, respectively. The figure describing 2050 population-weighted concentrations show M.V. population scenario.

Table A-6(a). Yearly Mean attribute number of cases *1000 (lower, upper of 95% CI) due to $PM_{2.5}$ exposures in January (assuming exposure * 12 months). Numbers larger than zero indicates cases attributed. Numbers less than zero imply cases avoided. Colors mark the future emission scenario: blue is Air, orange is Climate, green is SLCP and grey is MTFR

Health endpoints	Present emission scenario	Future emission scenario	Population projections							
			Medium variant	High variant	Low variant	Constant fertility	Instant replacement	Zero migration	Constant mortality	No change
Acute mortality	REAS	Air	-201 (-156, -1907)	-222 (-172, -2102)	-182 (-141, -1723)	-195 (-151, -1845)	-226 (-175, -2139)	-203 (-144, -1758)	-186 (-144, -1758)	-147 (-114, -1427)
		Climate	-253 (-196, -2322)	-279 (-217, -2560)	-229 (-178, -2099)	-245 (-190, -2247)	-284 (-220, -2605)	-256 (-199, -2346)	-234 (-181, -2141)	-200 (-155, -1863)
		SLCP	-256 (-198, -2340)	-282 (-219, -2580)	-231 (-179, -2114)	-247 (-192, -2264)	-287 (-222, -2625)	-258 (-200, -2364)	-236 (-183, -2157)	-202 (-156, -1881)
		MTFR	-344 (-267, -2978)	-380 (-295, -3284)	-311 (-242, -2692)	-333 (-259, -2882)	-386 (-300, -3341)	-348 (-270, -3009)	-317 (-247, -2746)	-291 (-226, -2543)
	MEIC	Air	-240 (-186, -2218)	-265 (-205, -2446)	-217 (-168, -2005)	-232 (-180, -2146)	-269 (-209, -2489)	-242 (-188, -2241)	-221 (-172, -2046)	-182 (-141, -1720)
		Climate	-292 (-226, -2610)	-322 (-250, -2878)	-264 (-205, -2359)	-282 (-219, -2525)	-327 (-254, -2928)	-295 (-229, -2637)	-269 (-209, -2407)	-234 (-181, -2131)
		SLCP	-294 (-228, -2627)	-324 (-252, -2896)	-266 (-206, -2374)	-285 (-221, -2542)	-330 (-256, -2947)	-297 (-231, -2654)	-271 (-210, -2422)	-236 (-183, -2148)
		MTFR	-382 (-297, -3229)	-421 (-327, -3560)	-345 (-268, -2918)	-370 (-287, -3125)	-429 (-333, -3623)	-386 (-300, -3262)	-352 (-274, -2978)	-325 (-252, -2773)

	EDGAR	Air	-14 (-11, -152)	-16 (-12, -168)	-13 (-10, -138)	-14 (-11, -147)	-16 (-12, -171)	-14 (-11, -154)	-13 (-10, -140)	20 (16, 222)
		Climate	-68 (-52, -700)	-75 (-58, -772)	-61 (-47, -632)	-66 (-51, -677)	-76 (-59, -785)	-68 (-53, -707)	-62 (-48, -645)	-34 (-26, -353)
		SLCP	-70 (-54, -723)	-77 (-60, -797)	-63 (-49, -653)	-68 (-52, -700)	-79 (-61, -811)	-71 (-55, -730)	-65 (-50, -667)	-36 (-28, -377)
		MTFR	-161 (-125, -1565)	-177 (-137, -1726)	-145 (-113, -1414)	-156 (-121, -1514)	-181 (-140, -1756)	-163 (-126, -1581)	-148 (-115, -1443)	-127 (-98, -1250)
Chronic mortality	REAS	Air	-1141 (-308, -2072)	-1258 (-339, -2285)	-1031 (-278, -1873)	-1104 (-298, -2005)	-1280 (-345, -2325)	-1152 (-311, -2094)	-1052 (-284, -1911)	-844 (-225, -1555)
		Climate	-1411 (-387, -2515)	-1556 (-426, -2773)	-1275 (-349, -2273)	-1365 (-374, -2433)	-1583 (-434, -2821)	-1425 (-391, -2540)	-1301 (-357, -2319)	-1122 (-305, -2022)
		SLCP	-1423 (-390, -2533)	-1569 (-430, -2793)	-1286 (-353, -2289)	-1377 (-377, -2451)	-1596 (-438, -2842)	-1437 (-394, -2559)	-1312 (-360, -2336)	-1134 (-308, -2041)
		MTFR	-1859 (-524, -3206)	-2049 (-577, -3535)	-1680 (-473, -2897)	-1799 (-507, -3102)	-2085 (-587, -3597)	-1878 (-529, -3239)	-1714 (-483, -2956)	-1579 (-442, -2741)
	MEIC	Air	-1343 (-366, -2404)	-1480 (-404, -2651)	-1213 (-331, -2173)	-1299 (-355, -2326)	-1506 (-411, -2697)	-1356 (-370, -2429)	-1238 (-338, -2217)	-1030 (-278, -1868)
		Climate	-1604 (-445, -2819)	-1769 (-490, -3108)	-1450 (-402, -2548)	-1552 (-430, -2728)	-1800 (-499, -3163)	-1621 (-449, -2848)	-1479 (-410, -2600)	-1299 (-357, -2306)
		SLCP	-1616 (-448, -2837)	-1781 (-494, -3128)	-1460 (-405, -2564)	-1563 (-434, -2745)	-1812 (-503, -3182)	-1632 (-453, -2866)	-1490 (-413, -2616)	-1310 (-360, -2325)

		MTFR	-2038 (-580, -3468)	-2247 (-640, -3823)	-1841 (-525, -3134)	-1972 (-562, -3355)	-2286 (-651, -3890)	-2058 (-586, -3503)	-1879 (-535, -3198)	-1741 (-493, -2981)
	EDGAR	Air	-86 (-22, -168)	-95 (-24, -185)	-78 (-20, -152)	-83 (-21, -162)	-96 (-25, -188)	-87 (-22, -169)	-79 (-20, -155)	124 (31, 245)
		Climate	-402 (-104, -768)	-443 (-115, -847)	-363 (-94, -694)	-389 (-101, -743)	-451 (-117, -861)	-406 (-105, -776)	-370 (-96, -708)	-201 (-52, -388)
		SLCP	-415 (-108, -793)	-458 (-119, -874)	-375 (-97, -717)	-402 (-104, -767)	-466 (-121, -890)	-420 (-109, -801)	-383 (-99, -731)	-215 (-55, -415)
		MTFR	-925 (-246, -1706)	-1020 (-272, -1881)	-836 (-223, -1541)	-895 (-238, -1650)	-1038 (-276, -1914)	-934 (-249, -1723)	-853 (-227, -1573)	-735 (-195, -1364)
Cardiovascular hospital admission	REAS	Air	-348 (-118, -624)	-383 (-130, -688)	-314 (-106, -564)	-336 (-114, -604)	-390 (-132, -701)	-351 (-119, -631)	-320 (-109, -576)	-254 (-86, -459)
		Climate	-437 (-148, -781)	-481 (-164, -861)	-395 (-134, -706)	-423 (-144, -756)	-490 (-167, -876)	-441 (-150, -789)	-403 (-137, -720)	-344 (-117, -617)
		SLCP	-441 (-150, -788)	-486 (-165, -869)	-398 (-135, -712)	-426 (-145, -762)	-494 (-168, -884)	-445 (-151, -796)	-406 (-138, -727)	-348 (-118, -624)
		MTFR	-591 (-202, -1049)	-652 (-223, -1157)	-534 (-183, -948)	-572 (-196, -1015)	-663 (-227, -1177)	-597 (-204, -1060)	-545 (-187, -968)	-500 (-171, -888)
	MEIC	Air	-414 (-141, -741)	-456 (-155, -817)	-374 (-127, -670)	-400 (-136, -717)	-464 (-158, -831)	-418 (-142, -749)	-382 (-130, -683)	-314 (-106, -564)
		Climate	-502 (-171, -896)	-554 (-189, -987)	-454 (-155, -809)	-486 (-166, -866)	-564 (-192, -1005)	-507 (-173, -905)	-463 (-158, -826)	-403 (-137, -720)

		SLCP	-506 (-173, -902)	-558 (-190, -995)	-457 (-156, -815)	-490 (-167, -873)	-568 (-194, -1012)	-511 (-174, -911)	-467 (-159, -832)	-407 (-138, -727)
		MTFR	-656 (-225, -1160)	-723 (-248, -1279)	-592 (-203, -1048)	-634 (-218, -1122)	-735 (-252, -1301)	-662 (-227, -1171)	-605 (-207, -1069)	-557 (-191, -987)
	EDGAR	Air	-25 (-8, -45)	-27 (-9, -50)	-22 (-7, -41)	-24 (-8, -44)	-28 (-9, -51)	-25 (-8, -46)	-23 (-8, -42)	35 (12, 65)
		Climate	-118 (-39, -214)	-130 (-43, -236)	-106 (-36, -193)	-114 (-38, -207)	-132 (-44, -240)	-119 (-40, -216)	-108 (-36, -197)	-58 (-19, -106)
		SLCP	-122 (-41, -221)	-134 (-45, -244)	-110 (-37, -200)	-118 (-39, -214)	-136 (-46, -248)	-123 (-41, -223)	-112 (-38, -204)	-62 (-21, -114)
		MTFR	-278 (-94, -502)	-307 (-104, -553)	-252 (-85, -454)	-269 (-91, -486)	-312 (-105, -563)	-281 (-95, -507)	-257 (-87, -463)	-220 (-74, -397)
Respiratory hospital admission	REAS	Air	-603 (-386, -810)	-665 (-426, -894)	-545 (-349, -732)	-584 (-374, -784)	-677 (-433, -909)	-610 (-390, -819)	-556 (-356, -747)	-445 (-283, -599)
		Climate	-752 (-483, -1004)	-829 (-533, -1107)	-679 (-437, -907)	-727 (-468, -972)	-843 (-542, -1127)	-759 (-488, -1014)	-693 (-446, -926)	-595 (-382, -798)
		SLCP	-758 (-488, -1012)	-836 (-538, -1116)	-685 (-441, -915)	-733 (-472, -980)	-850 (-547, -1136)	-766 (-493, -1023)	-699 (-450, -934)	-602 (-386, -806)
		MTFR	-1002 (-650, -1326)	-1105 (-717, -1462)	-905 (-588, -1199)	-969 (-629, -1283)	-1124 (-730, -1488)	-1012 (-657, -1340)	-924 (-600, -1223)	-849 (-550, -1126)
	MEIC	Air	-714 (-459, -955)	-787 (-506, -1053)	-645 (-414, -863)	-691 (-444, -924)	-801 (-514, -1071)	-721 (-463, -965)	-658 (-423, -881)	-545 (-349, -732)

		Climate	-859 (-555, -1143)	-947 (-611, -1260)	-776 (-501, -1033)	-831 (-537, -1106)	-963 (-622, -1282)	-868 (-560, -1155)	-792 (-511, -1054)	-693 (-446, -924)
		SLCP	-865 (-559, -1151)	-954 (-616, -1269)	-782 (-505, -1040)	-837 (-541, -1114)	-970 (-627, -1291)	-874 (-564, -1163)	-798 (-515, -1061)	-699 (-450, -933)
		MTFR	-1104 (-719, -1456)	-1217 (-793, -1605)	-997 (-650, -1315)	-1068 (-696, -1408)	-1238 (-807, -1633)	-1115 (-727, -1470)	-1018 (-663, -1342)	-941 (-612, -1243)
	EDGAR	Air	-44 (-28, -61)	-49 (-31, -67)	-40 (-25, -55)	-43 (-27, -59)	-50 (-31, -68)	-45 (-28, -61)	-41 (-26, -56)	64 (40, 87)
		Climate	-209 (-132, -284)	-230 (-145, -313)	-189 (-119, -257)	-202 (-128, -275)	-234 (-148, -319)	-211 (-133, -287)	-193 (-122, -262)	-104 (-65, -142)
		SLCP	-216 (-136, -294)	-238 (-150, -324)	-195 (-123, -266)	-209 (-132, -284)	-242 (-153, -330)	-218 (-138, -297)	-199 (-126, -271)	-111 (-70, -152)
		MTFR	-487 (-310, -656)	-537 (-342, -724)	-440 (-280, -593)	-471 (-300, -635)	-546 (-348, -736)	-492 (-313, -663)	-449 (-286, -605)	-386 (-245, -521)
Outpatient visits, all-causes	REAS	Air	-77458 (-48093, -102497)	-85403 (-53026, -113010)	-70000 (-43462, -92628)	-74946 (-46533, -99173)	-86897 (-53953, -114987)	-78250 (-48585, -103545)	-71424 (-44346, -94512)	-56577 (-35108, -74902)
		Climate	-97666 (-60690, -129146)	-107684 (-66915, -142392)	-88262 (-54846, -116710)	-94499 (-58722, -124958)	-109568 (-68086, -144884)	-98665 (-61311, -130466)	-90058 (-55962, -119085)	-76841 (-47727, -101648)
		SLCP	-98555 (-61245, -130317)	-108664 (-67527, -143683)	-89065 (-55348, -117769)	-95359 (-59259, -126091)	-110565 (-68708, -146198)	-99563 (-61871, -131649)	-90877 (-56474, -120165)	-77732 (-48282, -102824)

	MTFR	-133018 (-82779, -175672)	-146661 (-91270, -193690)	-120210 (-74808, -158756)	-128705 (-80095, -169976)	-149228 (-92867, -197080)	-134378 (-83626, -177468)	-122656 (-76330, -161987)	-112263 (-69843, -148298)
MEIC	Air	-92475 (-57452, -122303)	-101960 (-63345, -134848)	-83570 (-51920, -110527)	-89476 (-55589, -118337)	-103744 (-64453, -137207)	-93420 (-58039, -123554)	-85271 (-52976, -112776)	-69990 (-43458, -92611)
	Climate	-112617 (-70024, -148837)	-124168 (-77206, -164103)	-101773 (-63281, -134505)	-108965 (-67754, -144011)	-126341 (-78557, -166974)	-113769 (-70740, -150359)	-103844 (-64569, -137242)	-90187 (-56051, -119241)
	SLCP	-113503 (-70578, -150003)	-125145 (-77817, -165389)	-102574 (-63782, -135559)	-109823 (-68289, -145139)	-127335 (-79178, -168283)	-114664 (-71299, -151537)	-104661 (-65079, -138317)	-91076 (-56606, -120411)
	MTFR	-147854 (-92068, -195162)	-163019 (-101512, -215180)	-133617 (-83203, -176370)	-143059 (-89083, -188834)	-165871 (-103288, -218945)	-149365 (-93010, -197158)	-136336 (-84896, -179959)	-125495 (-78123, -165690)
EDGAR	Air	-5450 (-3374, -7230)	-6009 (-3720, -7971)	-4925 (-3049, -6533)	-5273 (-3264, -6995)	-6114 (-3785, -8111)	-5505 (-3408, -7303)	-5025 (-3111, -6666)	7741 (4789, 10274)
	Climate	-25973 (-16093, -34432)	-28637 (-17743, -37963)	-23472 (-14543, -31116)	-25131 (-15571, -33315)	-29139 (-18054, -38628)	-26239 (-16257, -34784)	-23950 (-14839, -31749)	-12839 (-7951, -17027)
	SLCP	-26876 (-16653, -35627)	-29633 (-18361, -39282)	-24288 (-15049, -32197)	-26005 (-16113, -34472)	-30151 (-18682, -39969)	-27151 (-16823, -35992)	-24782 (-15355, -32852)	-13744 (-8512, -18227)
	MTFR	-61877 (-38394, -81924)	-68224 (-42332, -90327)	-55919 (-34697, -74036)	-59871 (-37149, -79268)	-69417 (-43073, -91908)	-62510 (-38787, -82762)	-57057 (-35403, -75542)	-48815 (-30280, -64646)

Table A-6(b). Yearly Mean attribute number of cases *1000 (lower, upper of 95% CI) due to $PM_{2.5}$ exposures in July (assuming exposure * 12 months). Numbers larger than zero indicates cases attributed. Numbers less than zero imply cases avoided. Colors mark the future emission scenario: blue is Air, orange is Climate, green is SLCP and grey is MTFR

Health endpoints	Present emission scenario	Future emission scenario	Population projections							
			Medium variant	High variant	Low variant	Constant fertility	Instant replacement	Zero migration	Constant mortality	No change
Acute mortality	REAS	Air	-75 (-58, -774)	-83 (-64, -853)	-68 (-53, -700)	-73 (-56, -749)	-84 (-65, -868)	-76 (-54, -714)	-69 (-54, -714)	-46 (-36, -482)
		Climate	-111 (-86, -1119)	-123 (-95, -1234)	-101 (-78, -1011)	-108 (-83, -1083)	-125 (-97, -1256)	-113 (-87, -1131)	-103 (-80, -1032)	-82 (-64, -838)
		SLCP	-109 (-85, -1100)	-121 (-93, -1212)	-99 (-76, -994)	-106 (-82, -1064)	-123 (-95, -1234)	-110 (-85, -1111)	-101 (-78, -1014)	-80 (-62, -817)
		MTFR	-178 (-138, -1711)	-196 (-152, -1887)	-161 (-125, -1546)	-172 (-133, -1656)	-200 (-155, -1920)	-180 (-139, -1729)	-164 (-127, -1578)	-149 (-115, -1443)
	MEIC	Air	-56 (-43, -581)	-62 (-48, -641)	-50 (-39, -525)	-54 (-42, -563)	-63 (-48, -652)	-56 (-44, -587)	-51 (-40, -536)	-29 (-22, -304)
		Climate	-92 (-71, -936)	-102 (-79, -1033)	-83 (-64, -846)	-89 (-69, -906)	-103 (-80, -1051)	-93 (-72, -946)	-85 (-66, -864)	-65 (-50, -670)
		SLCP	-90 (-70, -916)	-99 (-77, -1010)	-81 (-63, -828)	-87 (-67, -887)	-101 (-78, -1028)	-91 (-70, -926)	-83 (-64, -845)	-63 (-49, -650)
		MTFR	-159 (-123, -1546)	-175 (-135, -1704)	-143 (-111, -1397)	-154 (-119, -1496)	-178 (-138, -1734)	-160 (-124, -1561)	-146 (-113, -1425)	-132 (-102, -1293)
	EDGAR	Air	41 (32, 454)	45 (35, 500)	37 (28, 410)	40 (31, 439)	46 (35, 509)	41 (32, 458)	38 (29, 418)	58 (44, 650)
		Climate	4 (3, 45)	5 (4, 49)	4 (3, 40)	4 (3, 43)	5 (4, 50)	4 (3, 45)	4 (3, 41)	21 (16, 228)

		SLCP	6 (5, 68)	7 (5, 75)	6 (4, 61)	6 (5, 66)	7 (5, 76)	6 (5, 68)	6 (4, 63)	23 (18, 252)
		MTFR	-63 (-49, -657)	-70 (-54, -724)	-57 (-44, -594)	-61 (-47, -636)	-71 (-55, -737)	-64 (-50, -664)	-58 (-45, -606)	-47 (-36, -489)
Chronic mortality	REAS	Air	-445 (-116, -849)	-491 (-127, -936)	-403 (-104, -767)	-431 (-112, -821)	-500 (-130, -952)	-450 (-117, -857)	-411 (-107, -783)	-275 (-71, -529)
		Climate	-651 (-171, -1224)	-718 (-188, -1349)	-589 (-154, -1106)	-630 (-165, -1184)	-731 (-192, -1373)	-658 (-173, -1236)	-601 (-158, -1129)	-485 (-126, -917)
		SLCP	-639 (-168, -1203)	-705 (-185, -1326)	-578 (-152, -1087)	-619 (-162, -1164)	-717 (-188, -1349)	-646 (-169, -1215)	-590 (-155, -1109)	-473 (-123, -895)
		MTFR	-1016 (-272, -1863)	-1121 (-300, -2054)	-918 (-246, -1683)	-983 (-263, -1802)	-1140 (-305, -2090)	-1027 (-275, -1882)	-937 (-251, -1717)	-854 (-228, -1572)
	MEIC	Air	-333 (-86, -638)	-367 (-95, -704)	-300 (-78, -577)	-322 (-83, -618)	-373 (-96, -716)	-336 (-87, -645)	-307 (-79, -589)	-173 (-44, -334)
		Climate	-542 (-141, -1026)	-597 (-156, -1131)	-490 (-128, -927)	-524 (-137, -992)	-608 (-159, -1151)	-547 (-143, -1036)	-500 (-130, -946)	-385 (-100, -735)
		SLCP	-530 (-138, -1004)	-584 (-152, -1107)	-479 (-125, -907)	-513 (-134, -971)	-594 (-155, -1126)	-535 (-140, -1014)	-488 (-127, -926)	-373 (-97, -713)
		MTFR	-913 (-243, -1685)	-1006 (-268, -1858)	-825 (-220, -1523)	-883 (-235, -1630)	-1024 (-273, -1890)	-922 (-246, -1702)	-842 (-224, -1553)	-761 (-202, -1410)
	EDGAR	Air	252 (63, 502)	277 (69, 553)	227 (57, 453)	243 (61, 485)	282 (71, 563)	254 (64, 507)	232 (58, 462)	358 (89, 720)
		Climate	25 (6, 49)	28 (7, 54)	23 (6, 44)	24 (6, 48)	28 (7, 55)	25 (6, 50)	23 (6, 45)	127 (32, 252)
		SLCP	38 (10, 75)	42 (11, 82)	34 (9, 68)	37 (9, 72)	43 (11, 84)	38 (10, 76)	35 (9, 69)	140 (35, 278)

		MTFR	-377 (-97, -721)	-415 (-107, -795)	-340 (-88, -651)	-364 (-94, -697)	-422 (-109, -809)	-380 (-98, -728)	-347 (-90, -665)	-279 (-72, -537)
Cardiovascular hospital admission	REAS	Air	-131 (-44, -237)	-144 (-48, -262)	-118 (-40, -214)	-126 (-42, -230)	-147 (-49, -266)	-132 (-44, -240)	-120 (-40, -219)	-80 (-27, -146)
		Climate	-193 (-65, -350)	-213 (-72, -386)	-174 (-59, -316)	-187 (-63, -338)	-217 (-73, -392)	-195 (-66, -353)	-178 (-60, -322)	-143 (-48, -259)
		SLCP	-189 (-64, -343)	-209 (-70, -378)	-171 (-58, -310)	-183 (-62, -332)	-213 (-72, -385)	-191 (-64, -347)	-175 (-59, -316)	-139 (-47, -253)
		MTFR	-307 (-104, -554)	-339 (-115, -610)	-278 (-94, -500)	-297 (-101, -536)	-345 (-117, -621)	-311 (-105, -559)	-283 (-96, -510)	-258 (-87, -464)
	MEIC	Air	-97 (-32, -176)	-107 (-36, -194)	-88 (-29, -159)	-94 (-31, -171)	-109 (-36, -198)	-98 (-33, -178)	-89 (-30, -163)	-50 (-17, -91)
		Climate	-160 (-54, -290)	-176 (-59, -319)	-144 (-49, -262)	-154 (-52, -280)	-179 (-60, -325)	-161 (-54, -293)	-147 (-49, -267)	-113 (-38, -205)
		SLCP	-156 (-52, -283)	-172 (-58, -312)	-141 (-47, -256)	-151 (-51, -274)	-175 (-59, -318)	-158 (-53, -286)	-144 (-48, -261)	-109 (-37, -199)
		MTFR	-274 (-93, -495)	-303 (-102, -546)	-248 (-84, -447)	-266 (-90, -479)	-308 (-104, -555)	-277 (-94, -500)	-253 (-85, -456)	-228 (-77, -412)
	EDGAR	Air	71 (24, 131)	78 (26, 144)	64 (21, 118)	69 (23, 126)	80 (27, 147)	72 (24, 132)	66 (22, 120)	101 (33, 185)
		Climate	7 (2, 13)	8 (3, 14)	6 (2, 12)	7 (2, 13)	8 (3, 15)	7 (2, 13)	7 (2, 12)	36 (12, 66)
		SLCP	11 (4, 20)	12 (4, 22)	10 (3, 18)	11 (4, 19)	12 (4, 22)	11 (4, 20)	10 (3, 18)	40 (13, 73)

		MTFR	-110 (-37, -200)	-121 (-41, -221)	-99 (-33, -181)	-106 (-36, -194)	-123 (-41, -224)	-111 (-37, -202)	-101 (-34, -184)	-81 (-27, -148)
Respiratory hospital admission	REAS	Air	-232 (-146, -315)	-256 (-161, -348)	-209 (-132, -285)	-224 (-142, -305)	-260 (-164, -354)	-234 (-148, -318)	-214 (-135, -291)	-143 (-90, -195)
		Climate	-341 (-216, -462)	-375 (-238, -509)	-308 (-195, -417)	-329 (-209, -447)	-382 (-242, -518)	-344 (-218, -466)	-314 (-199, -426)	-253 (-160, -343)
		SLCP	-334 (-212, -453)	-369 (-234, -500)	-302 (-191, -409)	-323 (-205, -438)	-375 (-238, -508)	-338 (-214, -458)	-308 (-195, -418)	-246 (-156, -335)
		MTFR	-536 (-342, -722)	-591 (-377, -796)	-484 (-309, -652)	-519 (-331, -698)	-601 (-384, -810)	-542 (-346, -729)	-494 (-315, -665)	-450 (-287, -606)
	MEIC	Air	-173 (-109, -235)	-190 (-120, -259)	-156 (-98, -213)	-167 (-105, -228)	-194 (-122, -264)	-174 (-110, -238)	-159 (-100, -217)	-89 (-56, -122)
		Climate	-283 (-179, -384)	-311 (-197, -423)	-255 (-162, -347)	-273 (-173, -371)	-317 (-200, -430)	-285 (-181, -388)	-261 (-165, -354)	-201 (-127, -273)
		SLCP	-276 (-175, -375)	-305 (-193, -414)	-250 (-158, -339)	-267 (-169, -363)	-310 (-196, -421)	-279 (-176, -379)	-255 (-161, -346)	-194 (-123, -264)
		MTFR	-480 (-306, -648)	-529 (-337, -714)	-434 (-276, -585)	-465 (-296, -627)	-539 (-343, -727)	-485 (-309, -654)	-443 (-282, -597)	-400 (-254, -540)
	EDGAR	Air	129 (80, 177)	142 (89, 196)	116 (73, 160)	125 (78, 172)	145 (90, 199)	130 (81, 179)	119 (74, 164)	183 (114, 252)
		Climate	13 (8, 18)	14 (9, 19)	12 (7, 16)	12 (8, 17)	14 (9, 20)	13 (8, 18)	12 (7, 16)	65 (41, 90)
		SLCP	20 (12, 27)	22 (14, 30)	18 (11, 24)	19 (12, 26)	22 (14, 30)	20 (12, 27)	18 (11, 25)	72 (45, 99)

		MTFR	-196 (-123, -266)	-216 (-136, -294)	-177 (-112, -241)	-189 (-119, -258)	-219 (-138, -299)	-198 (-125, -269)	-180 (-114, -246)	-145 (-91, -198)
Outpatient visits, all-causes	REAS	Air	-77458 (-48093, -102497)	-85403 (-53026, -113010)	-70000 (-43462, -92628)	-74946 (-46533, -99173)	-86897 (-53953, -114987)	-78250 (-48585, -103545)	-71424 (-44346, -94512)	-56577 (-35108, -74902)
		Climate	-28876 (-17893, -38276)	-31838 (-19729, -42202)	-26096 (-16170, -34590)	-27940 (-17313, -37035)	-32395 (-20074, -42940)	-29172 (-18076, -38667)	-26627 (-16499, -35294)	-17677 (-10950, -23438)
		SLCP	-42789 (-26530, -56690)	-47178 (-29251, -62505)	-38669 (-23975, -51231)	-41402 (-25669, -54852)	-48004 (-29763, -63599)	-43227 (-26801, -57270)	-39456 (-24463, -52274)	-31614 (-19595, -41895)
		MTFR	-41982 (-26028, -55622)	-46288 (-28698, -61327)	-37939 (-23522, -50266)	-40621 (-25184, -53818)	-47098 (-29200, -62400)	-42411 (-26294, -56191)	-38711 (-24000, -51289)	-30806 (-19093, -40825)
	MEIC	Air	-68425 (-42469, -90573)	-75443 (-46825, -99863)	-61837 (-38379, -81852)	-66206 (-41092, -87636)	-76764 (-47644, -101610)	-69125 (-42903, -91499)	-63095 (-39160, -83517)	-57282 (-35546, -75834)
		Climate	-21403 (-13258, -28378)	-23598 (-14618, -31288)	-19342 (-11982, -25645)	-20709 (-12829, -27457)	-24011 (-14874, -31836)	-21622 (-13394, -28668)	-19736 (-12226, -26167)	-11009 (-6817, -14601)
		SLCP	-35338 (-21903, -46831)	-38963 (-24150, -51634)	-31936 (-19794, -42322)	-34192 (-21193, -45312)	-39645 (-24572, -52538)	-35700 (-22127, -47310)	-32585 (-20197, -43183)	-24969 (-15471, -33097)
		MTFR	-34530 (-21401, -45761)	-38071 (-23596, -50454)	-31205 (-19341, -41354)	-33410 (-20707, -44277)	-38737 (-24009, -51337)	-34883 (-21620, -46228)	-31840 (-19734, -42196)	-24159 (-14969, -32025)
	EDGAR	Air	-61015 (-37858, -80786)	-67274 (-41741, -89072)	-55140 (-34213, -73007)	-59037 (-36631, -78166)	-68451 (-42472, -90631)	-61639 (-38245, -81612)	-56262 (-34909, -74492)	-50677 (-31438, -67108)
		Climate	15622 (9663, 20739)	17224 (10654, 22866)	14118 (8732, 18742)	15115 (9349, 20067)	17526 (10840, 23267)	15782 (9761, 20951)	14405 (8910, 19124)	22026 (13619, 29250)

SLCP	1576 (975, 2091)	1738 (1076, 2306)	1424 (882, 1890)	1525 (944, 2024)	1768 (1094, 2346)	1592 (985, 2113)	1453 (899, 1929)	7956 (4922, 10559)
MTFR	2391 (1480, 3173)	2637 (1632, 3499)	2161 (1337, 2868)	2314 (1432, 3070)	2683 (1660, 3560)	2416 (1495, 3206)	2205 (1365, 2926)	8772 (5427, 11643)

Table A-6(c). Yearly Mean attribute number of cases *1000 (lower, upper of 95% CI) due to O_3 exposures in January (assuming exposure * 12 months). Numbers larger than zero indicates cases attributed. Numbers less than zero imply cases avoided. Colors mark the future emission scenario: blue is Air, orange is Climate, green is SLCP and grey is MTFR

Health endpoints	Present emission scenario	Future emission scenario	Population projections							
			Medium variant	High variant	Low variant	Constant fertility	Instant replacement	Zero migration	Constant mortality	No change
Acute mortality	REAS	Air	141 (59, 219)	155 (65, 241)	127 (53, 198)	136 (57, 212)	158 (66, 245)	142 (54, 202)	130 (54, 202)	180 (75, 280)
		Climate	124 (52, 192)	136 (57, 212)	112 (47, 174)	120 (50, 186)	139 (58, 215)	125 (52, 194)	114 (48, 177)	162 (68, 253)
		SLCP	63 (26, 97)	69 (29, 107)	57 (24, 88)	61 (25, 94)	70 (29, 109)	63 (26, 98)	58 (24, 89)	101 (42, 157)
		MTFR	53 (22, 83)	59 (25, 91)	48 (20, 75)	52 (22, 80)	60 (25, 93)	54 (23, 84)	49 (21, 76)	92 (38, 143)
	MEIC	Air	192 (80, 299)	212 (88, 330)	173 (72, 270)	186 (77, 289)	215 (90, 335)	194 (81, 302)	177 (74, 276)	226 (94, 352)
		Climate	175 (73, 272)	193 (80, 300)	158 (66, 246)	169 (70, 263)	196 (82, 305)	176 (74, 275)	161 (67, 251)	208 (87, 325)
		SLCP	113 (47, 176)	125 (52, 194)	102 (43, 159)	110 (46, 170)	127 (53, 197)	114 (48, 178)	104 (44, 162)	146 (61, 228)
		MTFR	104 (44, 162)	115 (48, 178)	94 (39, 146)	101 (42, 156)	117 (49, 181)	105 (44, 163)	96 (40, 149)	137 (57, 214)
	EDGAR	Air	112 (47, 174)	123 (52, 192)	101 (42, 157)	108 (45, 168)	126 (53, 195)	113 (47, 176)	103 (43, 160)	154 (64, 240)
		Climate	95 (40, 147)	105 (44, 162)	86 (36, 133)	92 (38, 143)	107 (45, 165)	96 (40, 149)	88 (37, 136)	137 (57, 213)
		SLCP	34 (14, 53)	38 (16, 58)	31 (13, 48)	33 (14, 51)	38 (16, 59)	35 (14, 53)	32 (13, 49)	76 (32, 117)
		MTFR	25 (11, 39)	28 (12, 43)	23 (10, 35)	24 (10, 38)	28 (12, 44)	25 (11, 39)	23 (10, 36)	66 (28, 103)
Cardiovascular hospital admission	REAS	Air	682 (257, 1124)	752 (283, 1240)	616 (232, 1016)	660 (249, 1088)	765 (288, 1261)	689 (260, 1136)	629 (237, 1037)	883 (329, 1471)

	Climate	597 (226, 981)	658 (249, 1082)	539 (204, 887)	577 (218, 949)	669 (253, 1101)	603 (228, 991)	550 (208, 905)	795 (297, 1320)
	SLCP	298 (114, 485)	329 (126, 535)	270 (103, 438)	289 (110, 469)	335 (128, 544)	301 (115, 490)	275 (105, 447)	487 (184, 799)
	MTFR	254 (97, 413)	280 (107, 455)	230 (88, 373)	246 (94, 400)	285 (109, 463)	257 (98, 417)	234 (90, 381)	442 (168, 724)
MEIC	Air	940 (351, 1564)	1037 (387, 1725)	850 (318, 1414)	910 (340, 1514)	1055 (394, 1755)	950 (355, 1580)	867 (324, 1442)	1121 (414, 1885)
	Climate	853 (320, 1414)	940 (352, 1559)	771 (289, 1278)	825 (309, 1368)	957 (358, 1587)	861 (323, 1429)	786 (295, 1304)	1030 (382, 1726)
	SLCP	546 (207, 896)	602 (228, 987)	493 (187, 809)	528 (200, 867)	612 (232, 1005)	551 (209, 905)	503 (191, 826)	714 (268, 1182)
	MTFR	500 (190, 820)	552 (209, 904)	452 (172, 741)	484 (184, 793)	561 (213, 920)	506 (192, 828)	461 (175, 756)	667 (251, 1103)
EDGAR	Air	539 (204, 885)	595 (225, 976)	488 (185, 800)	522 (198, 856)	605 (229, 993)	545 (206, 894)	497 (188, 816)	751 (282, 1246)
	Climate	456 (173, 745)	502 (191, 822)	412 (156, 674)	441 (168, 721)	511 (194, 836)	460 (175, 753)	420 (160, 687)	665 (250, 1099)
	SLCP	162 (62, 262)	179 (69, 289)	146 (56, 237)	157 (60, 254)	182 (70, 294)	164 (63, 265)	149 (57, 242)	362 (138, 591)
	MTFR	119 (46, 192)	131 (50, 211)	107 (41, 173)	115 (44, 186)	133 (51, 215)	120 (46, 194)	109 (42, 177)	318 (121, 518)

Respiratory hospital admission	REAS	Air	800 (536, 1073)	882 (591, 1184)	723 (484, 970)	774 (518, 1039)	897 (601, 1204)	808 (541, 1084)	737 (494, 990)	1048 (695, 1420)
		Climate	698 (469, 934)	769 (517, 1030)	630 (423, 844)	675 (453, 904)	783 (526, 1048)	705 (473, 943)	643 (432, 861)	940 (626, 1269)
		SLCP	345 (234, 457)	380 (258, 504)	311 (211, 413)	333 (226, 442)	387 (262, 513)	348 (236, 462)	318 (215, 421)	568 (382, 759)
		MTFR	293 (199, 388)	323 (219, 428)	265 (180, 351)	284 (193, 376)	329 (223, 436)	296 (201, 392)	270 (184, 358)	514 (347, 686)
	MEIC	Air	1114 (740, 1507)	1228 (816, 1662)	1007 (669, 1362)	1078 (716, 1458)	1250 (831, 1691)	1125 (748, 1523)	1027 (683, 1390)	1344 (885, 1836)
		Climate	1007 (671, 1358)	1110 (740, 1498)	910 (606, 1228)	974 (649, 1314)	1129 (753, 1524)	1017 (678, 1372)	928 (619, 1253)	1230 (813, 1676)
		SLCP	637 (428, 851)	702 (472, 938)	575 (387, 769)	616 (414, 823)	714 (480, 955)	643 (433, 860)	587 (395, 785)	841 (561, 1133)
		MTFR	583 (393, 778)	643 (433, 858)	527 (355, 703)	564 (380, 753)	654 (440, 873)	589 (397, 786)	537 (362, 717)	784 (525, 1055)
	EDGAR	Air	629 (423, 841)	694 (467, 927)	569 (383, 760)	609 (410, 814)	706 (475, 943)	636 (428, 849)	580 (390, 775)	887 (591, 1197)
		Climate	530 (357, 706)	584 (394, 778)	479 (323, 638)	513 (346, 683)	594 (401, 792)	535 (361, 713)	488 (330, 651)	782 (523, 1051)
		SLCP	186 (127, 246)	205 (140, 271)	168 (114, 222)	180 (123, 238)	209 (142, 276)	188 (128, 248)	172 (117, 227)	420 (284, 559)

		MTFR	136 (93, 179)	150 (102, 198)	123 (84, 162)	132 (90, 174)	153 (104, 201)	137 (94, 181)	125 (86, 165)	368 (249, 489)

Table A-6(d). Yearly Mean attribute number of cases *1000 (lower, upper of 95% CI) due to O_3 exposures in July(assuming exposure * 12 months). Numbers larger than zero indicates cases attributed. Numbers less than zero imply cases avoided. Colors mark the future emission scenario: blue is Air, orange is Climate, green is SLCP and grey is MTFR

Health endpoints	Present emission scenario	Future emission scenario	Population projections							
			Medium variant	High variant	Low variant	Constant fertility	Instant replacement	Zero migration	Constant mortality	No change
Acute mortality	REAS	Air	58 (24, 91)	64 (27, 100)	53 (22, 82)	57 (24, 88)	66 (27, 102)	59 (23, 84)	54 (23, 84)	119 (50, 184)
		Climate	15 (6, 24)	17 (7, 26)	14 (6, 22)	15 (6, 23)	17 (7, 27)	16 (7, 24)	14 (6, 22)	75 (31, 117)
		SLCP	-69 (-29, -106)	-76 (-32, -117)	-62 (-26, -96)	-67 (-28, -103)	-77 (-33, -119)	-70 (-29, -108)	-64 (-27, -98)	-10 (-4, -15)
		MTFR	-98 (-41, -152)	-109 (-46, -167)	-89 (-37, -137)	-95 (-40, -147)	-110 (-47, -170)	-99 (-42, -153)	-91 (-38, -140)	-40 (-17, -61)
	MEIC	Air	119 (50, 185)	131 (55, 203)	107 (45, 167)	115 (48, 179)	133 (56, 207)	120 (50, 186)	110 (46, 170)	173 (72, 269)
		Climate	75 (32, 117)	83 (35, 129)	68 (29, 106)	73 (31, 113)	85 (35, 131)	76 (32, 118)	70 (29, 108)	129 (54, 201)
		SLCP	-10 (-4, -15)	-11 (-4, -17)	-9 (-4, -14)	-9 (-4, -14)	-11 (-5, -17)	-10 (-4, -15)	-9 (-4, -14)	43 (18, 67)

		MTFR	-39 (-17, -61)	-43 (-18, -67)	-36 (-15, -55)	-38 (-16, -59)	-44 (-19, -68)	-40 (-17, -61)	-36 (-15, -56)	13 (6, 21)
	EDGAR	Air	110 (46, 171)	121 (51, 189)	100 (42, 155)	107 (45, 166)	124 (52, 192)	111 (47, 173)	102 (42, 158)	165 (69, 257)
		Climate	67 (28, 104)	74 (31, 114)	60 (25, 94)	65 (27, 100)	75 (31, 116)	68 (28, 105)	62 (26, 96)	122 (51, 189)
		SLCP	-18 (-8, -28)	-20 (-8, -31)	-16 (-7, -25)	-18 (-7, -27)	-20 (-9, -31)	-18 (-8, -28)	-17 (-7, -26)	36 (15, 55)
		MTFR	-48 (-20, -74)	-53 (-22, -81)	-43 (-18, -67)	-46 (-19, -71)	-54 (-23, -83)	-48 (-20, -75)	-44 (-19, -68)	6 (2, 9)
Cardiovascular hospital admission	REAS	Air	278 (106, 452)	307 (117, 499)	251 (96, 409)	269 (103, 438)	312 (119, 508)	281 (108, 457)	257 (98, 417)	574 (217, 946)
		Climate	73 (28, 118)	80 (31, 130)	66 (25, 106)	70 (27, 114)	82 (31, 132)	74 (28, 119)	67 (26, 108)	360 (137, 589)
		SLCP	-320 (-125, -509)	-353 (-138, -561)	-289 (-113, -460)	-309 (-121, -492)	-359 (-140, -571)	-323 (-126, -514)	-295 (-115, -469)	-46 (-18, -75)
		MTFR	-453 (-178, -718)	-500 (-196, -791)	-410 (-161, -648)	-439 (-172, -694)	-509 (-200, -805)	-458 (-180, -725)	-418 (-164, -662)	-184 (-72, -295)
	MEIC	Air	573 (217, 941)	632 (239, 1038)	518 (196, 851)	554 (210, 911)	643 (243, 1056)	579 (219, 951)	528 (200, 868)	848 (317, 1411)
		Climate	361 (137, 588)	397 (152, 648)	326 (124, 531)	349 (133, 569)	404 (154, 659)	364 (139, 594)	332 (127, 542)	627 (236, 1034)
		SLCP	-45 (-18, -73)	-50 (-19, -81)	-41 (-16, -66)	-44 (-17, -71)	-51 (-20, -82)	-46 (-18, -74)	-42 (-16, -67)	206 (79, 334)
		MTFR	-184 (-71, -294)	-203 (-79, -324)	-166 (-65, -265)	-178 (-69, -284)	-206 (-80, -329)	-186 (-72, -297)	-169 (-66, -271)	63 (24, 102)

	EDGAR	Air	531 (201, 870)	585 (222, 960)	480 (182, 787)	513 (195, 842)	595 (226, 976)	536 (203, 879)	489 (185, 803)	808 (302, 1344)
		Climate	319 (122, 520)	352 (134, 573)	288 (110, 470)	309 (118, 503)	358 (137, 583)	322 (123, 525)	294 (112, 479)	588 (222, 970)
		SLCP	-85 (-33, -136)	-94 (-36, -150)	-77 (-30, -123)	-82 (-32, -132)	-95 (-37, -153)	-86 (-33, -138)	-78 (-30, -126)	170 (65, 275)
		MTFR	-222 (-87, -355)	-245 (-96, -392)	-201 (-78, -321)	-215 (-84, -344)	-250 (-97, -398)	-225 (-88, -359)	-205 (-80, -327)	28 (11, 45)
Respiratory hospital admission	REAS	Air	321 (218, 426)	354 (240, 469)	290 (197, 385)	311 (211, 412)	360 (244, 478)	325 (220, 430)	296 (201, 393)	673 (451, 902)
		Climate	83 (57, 110)	92 (63, 121)	75 (51, 99)	81 (55, 106)	94 (64, 123)	84 (58, 111)	77 (53, 101)	418 (283, 556)
		SLCP	-360 (-249, -468)	-397 (-275, -516)	-325 (-225, -423)	-348 (-241, -453)	-404 (-279, -525)	-364 (-252, -473)	-332 (-230, -432)	-53 (-36, -69)
		MTFR	-508 (-353, -658)	-560 (-389, -725)	-459 (-319, -594)	-491 (-341, -636)	-570 (-396, -738)	-513 (-356, -664)	-468 (-325, -606)	-209 (-144, -272)
	MEIC	Air	669 (450, 895)	738 (496, 987)	605 (406, 809)	647 (435, 866)	751 (505, 1004)	676 (454, 904)	617 (415, 825)	1005 (668, 1360)
		Climate	417 (282, 555)	460 (311, 612)	377 (255, 501)	404 (273, 537)	468 (317, 622)	422 (285, 561)	385 (260, 512)	736 (493, 988)
		SLCP	-52 (-35, -68)	-57 (-39, -75)	-47 (-32, -61)	-50 (-34, -66)	-58 (-40, -76)	-52 (-36, -69)	-48 (-33, -63)	237 (161, 314)

	MTFR	-208 (-143, -272)	-229 (-158, -300)	-188 (-129, -246)	-201 (-139, -263)	-233 (-161, -305)	-210 (-145, -275)	-192 (-132, -251)	72 (49, 95)
EDGAR	Air	619 (416, 827)	682 (459, 911)	559 (376, 747)	599 (403, 800)	694 (467, 927)	625 (421, 835)	570 (384, 762)	957 (637, 1293)
	Climate	369 (250, 490)	407 (276, 540)	333 (226, 443)	357 (242, 474)	414 (280, 549)	373 (253, 495)	340 (231, 452)	690 (462, 925)
	SLCP	-97 (-66, -127)	-106 (-73, -140)	-87 (-60, -114)	-93 (-64, -122)	-108 (-74, -142)	-98 (-67, -128)	-89 (-61, -117)	195 (133, 258)
	MTFR	-252 (-173, -328)	-277 (-191, -362)	-227 (-157, -297)	-243 (-168, -318)	-282 (-195, -368)	-254 (-175, -332)	-232 (-160, -303)	32 (22, 42)

Table A-7(a). Analysis of variance result for estimation of national $PM_{2.5}$ –related acute mortality cases in January between 2008 and 2050. Numbers are round to the nearest hundredth

Source	Df	SS	MS	Percentage of total SS
present	2	8.99E+11	4.49E+11	74.04
future	3	2.59E+11	8.63E+10	21.33
pop	7	4.88E+10	6.98E+09	4.02
present x future	6	4.77E+07	7.95E+06	0.00
present x pop	14	6.00E+09	4.28E+08	0.49
future x pop	21	1.34E+09	6.38E+07	0.11
present x future x pop	42	2.47E+05	5.88E+03	0.00
Total	95	1.21E+12		100.00

Abbreviation: present, present emission scenarios; future: future emission scenarios; pop: population projections; SS: ANOVA Sum of squares; Df: degree of freedom; MS: mean squares;

Table A-7(b). Analysis of variance result for estimation of national $PM_{2.5}$ –related chronic mortality cases in January between 2008 and 2050. Numbers are round to the nearest hundredth

Source	Df	SS	MS	Percentage of total SS
present	2	2.59E+13	1.29E+13	74.73
future	3	7.03E+12	2.34E+12	20.31
pop	7	1.47E+12	2.10E+11	4.25
present x future	6	4.96E+10	8.27E+09	0.14
present x pop	14	1.61E+11	1.15E+10	0.47
future x pop	21	3.65E+10	1.74E+09	0.11
present x future x pop	42	2.58E+08	6.14E+06	0.00
Total	95	3.46E+13		100.00

Table A-7(c). Analysis of variance result for estimation of national $PM_{2.5}$–related Hospital Admission, Cardiovascular cases in January between 2008 and 2050. Numbers are round to the nearest hundredth

Source	Df	SS	MS	Percentage of total SS
present	2	2.65E+12	1.32E+12	74.13
future	3	7.58E+11	2.53E+11	21.21
pop	7	1.45E+11	2.07E+10	4.05
present x future	6	3.34E+08	5.57E+07	0.01
present x pop	14	1.75E+10	1.25E+09	0.49
future x pop	21	3.92E+09	1.87E+08	0.11
present x future x pop	42	1.73E+06	4.12E+04	0.00
Total	95	3.57E+12		100.00

Table A-7(d). Analysis of variance result for estimation of national $PM_{2.5}$–related Hospital Admission, respiratory cases in January between 2008 and 2050. Numbers are round to the nearest hundredth

Source	Df	SS	MS	Percentage of total SS
present	2	7.56E+12	3.78E+12	74.50
future	3	2.10E+12	7.00E+11	20.70
pop	7	4.22E+11	6.02E+10	4.16
present x future	6	6.65E+09	1.11E+09	0.07
present x pop	14	4.83E+10	3.45E+09	0.48
future x pop	21	1.09E+10	5.18E+08	0.11
present x future x pop	42	3.44E+07	8.20E+05	0.00
Total	95	1.01E+13		100.00

Table A-7(e). Analysis of variance result for estimation of national $PM_{2.5}$ –related outpatient visit cases in January between 2008 and 2050. Numbers are round to the nearest hundredth

Source	Df	SS	MS	Percentage of total SS
present	2	1.34E+17	6.72E+16	73.98
future	3	3.89E+16	1.30E+16	21.41
pop	7	7.27E+15	1.04E+15	4.01
present x future	6	2.62E+12	4.36E+11	0.00
present x pop	14	9.01E+14	6.44E+13	0.50
future x pop	21	2.01E+14	9.59E+12	0.11
present x future x pop	42	1.35E+10	3.23E+08	0.00
Total	95	1.82E+17		100.00

Table A-7(e). Analysis of variance result for estimation of national $PM_{2.5}$ –related acute mortality cases in July between 2008 and 2050. Numbers are round to the nearest hundredth

Source	Df	SS	MS	Percentage of total SS
present	2	2.40E+11	1.20E+11	62.05
future	3	1.35E+11	4.51E+10	35.01
pop	7	9.03E+09	1.29E+09	2.34
present x future	6	6.40E+06	1.07E+06	0.00
present x pop	14	1.61E+09	1.15E+08	0.42
future x pop	21	7.01E+08	3.34E+07	0.18
present x future x pop	42	3.32E+04	7.89E+02	0.00
Total	95	3.87E+11		100.00

Table A-7(f). Analysis of variance result for estimation of national $PM_{2.5}$ –related chronic mortality cases in July between 2008 and 2050. Numbers are round to the nearest hundredth

Source	Df	SS	MS	Percentage of total SS
present	2	8.20E+12	4.10E+12	62.84
future	3	4.46E+12	1.49E+12	34.16
pop	7	3.07E+11	4.39E+10	2.35
present x future	6	7.94E+09	1.32E+09	0.06
present x pop	14	5.27E+10	3.76E+09	0.40
future x pop	21	2.31E+10	1.10E+09	0.18
present x future x pop	42	4.11E+07	9.78E+05	0.00
Total	95	1.30E+13		100.00

Table A-7(f). Analysis of variance result for estimation of national $PM_{2.5}$ –related Hospital Admission, Cardiovascular cases in July between 2008 and 2050. Numbers are round to the nearest hundredth

Source	Df	SS	MS	Percentage of total SS
present	2	7.20E+11	3.60E+11	62.14
future	3	4.05E+11	1.35E+11	34.92
pop	7	2.71E+10	3.87E+09	2.34
present x future	6	4.57E+07	7.62E+06	0.00
present x pop	14	4.81E+09	3.43E+08	0.41
future x pop	21	2.10E+09	9.98E+07	0.18
present x future x pop	42	2.37E+05	5.63E+03	0.00
Total	95	1.16E+12		100.00

Table A-7(g). Analysis of variance result for estimation of national $PM_{2.5}$ –related Hospital Admission, respiratory cases in July between 2008 and 2050. Numbers are round to the nearest hundredth

Source	Df	SS	MS	Percentage of total SS
present	2	2.24E+12	1.12E+12	62.54
future	3	1.24E+12	4.12E+11	34.49
pop	7	8.41E+10	1.20E+10	2.35
present x future	6	9.93E+08	1.66E+08	0.03
present x pop	14	1.46E+10	1.04E+09	0.41
future x pop	21	6.39E+09	3.04E+08	0.18
present x future x pop	42	5.14E+06	1.22E+05	0.00
Total	95	3.58E+12		100.00

Table A-7(h). Analysis of variance result for estimation of national $PM_{2.5}$ –related outpatient visit cases in July between 2008 and 2050. Numbers are round to the nearest hundredth

Source	Df	SS	MS	Percentage of total SS
present	2	3.54E+16	1.77E+16	61.99
future	3	2.00E+16	6.67E+15	35.08
pop	7	1.33E+15	1.90E+14	2.33
present x future	6	3.46E+11	5.77E+10	0.00
present x pop	14	2.38E+14	1.70E+13	0.42
future x pop	21	1.04E+14	4.94E+12	0.18
present x future x pop	42	1.79E+09	4.27E+07	0.00
Total	95	5.70E+16		100.00

Table A-8(a). Analysis of variance result for estimation of national O_3–related acute mortality cases in January between 2008 and 2050. Numbers are round to the nearest hundredth

Source	Df	SS	MS	Percentage of total SS
present	2	1.02E+11	5.08E+10	38.96
future	3	1.38E+11	4.59E+10	52.82
pop	7	2.01E+10	2.87E+09	7.69
present x future	6	2.63E+06	4.39E+05	0.00
present x pop	14	6.70E+08	4.79E+07	0.26
future x pop	21	7.13E+08	3.40E+07	0.27
present x future x pop	42	1.36E+04	3.24E+02	0.00
Total	95	2.61E+11		100.00

Table A-8(b). Analysis of variance result for estimation of national O_3–related Hospital Admission, Cardiovascular cases in January between 2008 and 2050. Numbers are round to the nearest hundredth

Source	Df	SS	MS	Percentage of total SS
present	2	2.48E+12	1.24E+12	38.98
future	3	3.35E+12	1.12E+12	52.68
pop	7	4.97E+11	7.09E+10	7.81
present x future	6	1.12E+09	1.86E+08	0.02
present x pop	14	1.51E+10	1.08E+09	0.24
future x pop	21	1.75E+10	8.33E+08	0.28
present x future x pop	42	5.84E+06	1.39E+05	0.00
Total	95	6.36E+12		100.00

Table A-8(c). Analysis of variance result for estimation of national O_3–related Hospital Admission, respiratory cases in January between 2008 and 2050. Numbers are round to the nearest hundredth

Source	Df	SS	MS	Percentage of total SS
present	2	3.53E+12	1.76E+12	38.99
future	3	4.75E+12	1.58E+12	52.53
pop	7	7.17E+11	1.02E+11	7.92
present x future	6	4.52E+09	7.53E+08	0.05
present x pop	14	2.03E+10	1.45E+09	0.22
future x pop	21	2.55E+10	1.22E+09	0.28
present x future x pop	42	2.43E+07	5.78E+05	0.00
Total	95	9.05E+12		100.00

Table A-8(d). Analysis of variance result for estimation of national O_3–related acute mortality cases in July between 2008 and 2050. Numbers are round to the nearest hundredth

Source	Df	SS	MS	Percentage of total SS
present	2	6.55E+10	3.27E+10	13.36
future	3	3.89E+11	1.30E+11	79.47
pop	7	3.27E+10	4.67E+09	6.67
present x future	6	4.90E+06	8.17E+05	0.00
present x pop	14	4.30E+08	3.07E+07	0.09
future x pop	21	2.01E+09	9.59E+07	0.41
present x future x pop	42	2.54E+04	6.04E+02	0.00
Total	95	4.90E+11		100.00

Table A-8(d). Analysis of variance result for estimation of national O_3–related Hospital Admission, Cardiovascular cases in July between 2008 and 2050. Numbers are round to the nearest hundredth

Source	Df	SS	MS	Percentage of total SS
present	2	1.47E+12	7.33E+11	13.23
future	3	8.80E+12	2.93E+12	79.44
pop	7	7.55E+11	1.08E+11	6.82
present x future	6	1.91E+09	3.19E+08	0.02
present x pop	14	8.80E+09	6.29E+08	0.08
future x pop	21	4.62E+10	2.20E+09	0.42
present x future x pop	42	1.01E+07	2.39E+05	0.00
Total	95	1.11E+13		100.00

Table A-8(e). Analysis of variance result for estimation of national O_3 –related Hospital Admission, respiratory cases in July between 2008 and 2050. Numbers are round to the nearest hundredth

Source	Df	SS	MS	Percentage of total SS
present	2	1.93E+12	9.66E+11	13.10
future	3	1.17E+13	3.90E+12	79.37
pop	7	1.03E+12	1.47E+11	6.96
present x future	6	7.17E+09	1.20E+09	0.05
present x pop	14	1.08E+10	7.75E+08	0.07
future x pop	21	6.40E+10	3.05E+09	0.43
present x future x pop	42	3.93E+07	9.35E+05	0.00
Total	95	1.47E+13		100.00